PHILOSOPHICAL TRANSACTIONS OF THE ROYAL SOCIETY B BIOLOGICAL SCIENCES

Distribution of Receptors and Functions on Cell Surfaces: Quantitation of Ligand-Receptor Mobility and a New Model for the Control of Plasma Membrane Topography

Janet M. Oliver and R. D. Berlin

Phil. Trans. R. Soc. Lond. B 1982 **299**, 215-235
doi: 10.1098/rstb.1982.0128

Phil. Trans. R. Soc. Lond. B **299**, 215–235 (1982)
Printed in Great Britain

Distribution of receptors and functions on cell surfaces: quantitation of ligand–receptor mobility and a new model for the control of plasma membrane topography

By Janet M. Oliver and R. D. Berlin

Department of Physiology, University of Connecticut Health Center, Farmington, Connecticut 06032, *U.S.A.*

[Plates 1 and 2]

The long-range movements of membrane ligand–receptor complexes into surface caps and into the pseudopods of cells performing phagocyosis, the uropods of motile cells and the cleavage furrows of dividing cells appear to be analogous processes. A common mechanism to explain these movements must take into account several recent observations. First, laser photobleaching studies have indicated that Concanavalin A-receptor movement occurs unidirectionally; and analyses of Con A redistribution by quantitative video intensification microscopy (Quavim) have shown that movement may exceed the maximum rates measured for protein diffusion in membranes. These are the results predicted for a process of directed migration but not for a process of diffusion with entrapment. In addition it has been found that membrane receptors may segregate out of as well as into cap, pseudopod, uropod and cleavage furrow regions and that topographical heterogeneity on asymmetric cells is not restricted to membrane molecular determinants but extends to a range of endocytic functions and to a macromolecular complex, the coated pit. All dynamic surface events are arrested during mitosis. A new model for the regulation of plasma membrane topography has been developed from these diverse quantitative, functional and morphological data. Its essence is the entrainment of selected membrane determinants on membrane waves directed towards regions such as caps, pseudopods, uropods and cleavage furrows. The waves are initiated by tension due to asymmetric microfilament–membrane interaction.

Introduction

Many ligands that bind more or less uniformly to cell surface receptors are subsequently accumulated within a much smaller area of the surface. The redistribution of various lectins and antibodies into surface caps on leucocytes is perhaps the most familiar example. These caps usually occupy a bulge or protuberance at one pole of the cell. The same ligand–receptor complexes are also redistributed into pseudopods during phagocytosis, into uropods during chemotaxis, and into the cleavage furrows of dividing cells (reviewed in Oliver & Berlin 1982; Berlin & Oliver 1982). These predictable topographical patterns are illustrated for Concanavalin A–receptor complexes in figure 1.

How do such movements occur? Among the many hypotheses developed to explain capping processes, the simplest is the free diffusion of ligand-receptor complexes and their accumulation by cross-linking or by immobilization in a 'trap' over some region of the cell (see, for example, Schreiner & Unanue 1976). New physical techniques, particularly the measurement of fluorescence recovery after photobleaching (Frap), have now allowed direct determinations of the rates of diffusional movement of surface constituents or ligand–receptor complexes (Cherry

1979). The data obtained so far indicate that the rates of protein diffusion in the two-dimensional plane of the membrane are slower in animal cell membranes than in free solution. Measured diffusion constants, D, usually range from 5×10^{-9} to 10^{-11} cm^2 s^{-1} (or slower) for proteins or ligand–protein receptor complexes. It has also been found that diffusion is usually isotropic. In one system faster diffusion rates were measured along one cell axis than along another,

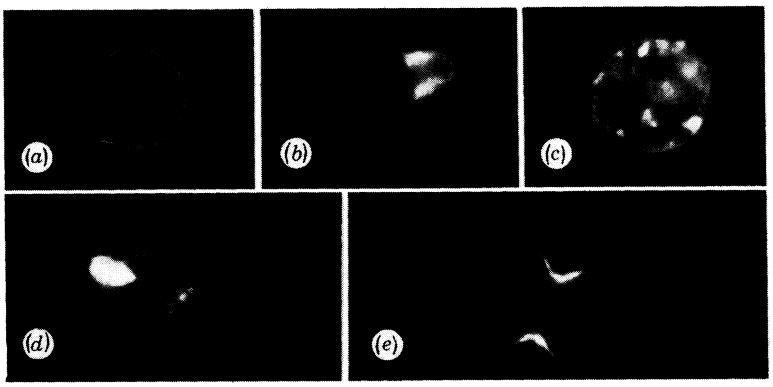

FIGURE 1. The distribution of Con A–receptor complexes on cell surfaces. Variously treated cells were incubated for 5 min at 37 °C with fluorescein-conjugated Concanavalin A (F-Con A) (about 10 μg ml^{-1}). Lectin remains uniformly distributed on untreated cells (*a*). It accumulates in caps on microtubule-depleted (protuberant) cells (*b*), in the pseudopodia of cells performing phagocytosis (*c*), in the uropods of locomoting cells (*d*) and in the cleavage furrow during cytokinesis (*e*). All cells are human polymorphonuclear leukocytes (p.m.ns) except for the mitotic, which is a Chinese hamster ovary cell.

indicating that an anisotropic process may occur in special cases (Smith *et al.* 1979). Diffusion is never unidirectional, however, by definition.

Recent studies, summarized below, establish that the movement of Concanavalin A–receptor complexes (and probably other ligand–receptor complexes) into the cleavage furrows of dividing cells, the caps of colchicine-treated (protuberant) cells and the uropods of locomoting cells occurs at rates at or beyond the probable limits of diffusion and *is* unidirectional. These results rule out the diffusion mechanism and point towards some form of membrane flow.

Other studies, also reviewed below, establish that the sites of Con A–receptor complex accumulation share common ultrastructural features, particularly the accumulation of submembranous microfilaments. Furthermore, a variety of additional determinants of membrane structure (Fc and C_3b receptors, coated pits) and function (fluid and adsorptive pinocytosis) are distributed in asymmetric patterns with respect to these regions. Indeed we have identified only one receptor, the GM1 ganglioside receptor for the B fragment of choleratoxin, whose distribution appears to remain random in the presence of ligand during cytokinesis, capping and related processes.

A new model to explain the predictable long-range movement of membrane receptors and ligand–receptor complexes into cap and analogous membranes has been developed from these qualitative and quantitative data.

PHILOSOPHICAL TRANSACTIONS OF THE ROYAL SOCIETY B BIOLOGICAL SCIENCES

Quantitative analysis of ligand–receptor movement: methods

Two independent methods have been applied to the quantitative analysis of the redistribution of bound Con A on cell surfaces. The first method was developed by Koppel (1979) with modifications as described in detail by Koppel *et al.* (1982). It involves the use of a series of high-resolution multipoint fluorescence scans to follow the distribution of surface label on selected cells as a function of time. These scans are generated by first focusing an attenuated

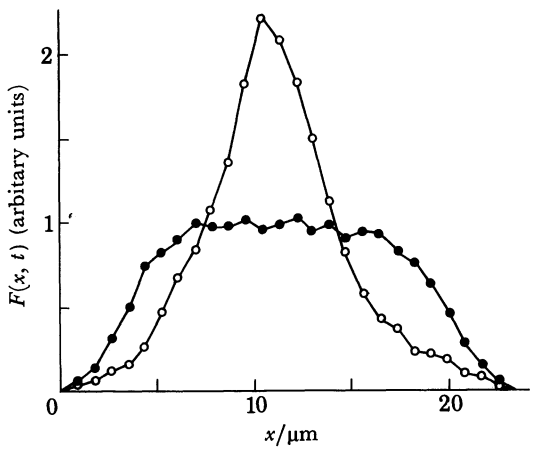

Figure 2. Typical laser-fluorescence scans of FS-Con A distribution across the long axis of a mitotic J774 macrophage in early anaphase (●), and 7 min later in telophase (○). Geometrical 'edge effects' were minimized by focusing the laser beam to a narrow line on the sample perpendicular to the scan axis. The cell was incubated with FS-Con A at 100 μg ml^{-1} for 2 min at room temperature. Fluorescence redistribution was followed at 37 °C.

laser beam from an argon-ion laser ($\lambda = 488$ nm) through the incident-light illuminator of the microscope either to a small spot on the cell or (with the use of a cylindrical lens) to a narrow line perpendicular to the scan axis and then moving the beam along a linear axis by a galvanometric scanning mirror. In cells undergoing cytokinesis, the selected axis usually runs perpendicular to the cleavage furrow through the poles. $F(x, t)$, the fluorescence intensity as a function of distance along the pole-to-pole axis at time t after initiation of redistribution, is detected by a thermoelectrically cooled photomultiplier tube and quantified with photon-counting electronics synchronized to the position of the scanning laser beam. The optical apparatus and electronics are described in detail elsewhere (Koppel 1979). Figure 2 shows two typical laser line scans across a dividing cell labelled with fluorescein-conjugated succinyl Concanavalin A (FS-Con A), the first taken at the onset of anaphase and the second 7 min later in late telophase, showing the redistribution of lectin into the cleavage furrow.

This instrumentation permits the direct measurement of diffusion rates of fluorescence-tagged membrane markers by the method of fluorescence recovery after photobleaching (Frap). As illustrated below, intense bleaching pulses are generated by electronic switching to an alternative light path for the laser beam that avoids the attenuating pathway used for fluorescence monitoring. The attenuated beam is employed to record the increase in $F(x, t)$ as fluorophore diffuses back into the bleached region. Translational diffusion coefficients are then estimated from the rate of fluorescence recovery (Koppel 1979).

PHILOSOPHICAL TRANSACTIONS OF THE ROYAL SOCIETY B BIOLOGICAL SCIENCES

Results obtained by this procedure have provided the first quantitative information essential to distinguish flow from diffusional models of receptor redistribution. On the other hand, the technique has several limitations. One is the requirement for cells to remain fixed in space (usually possible during cytokinesis but essentially incompatible with processes like capping or chemotaxis). Other problems include the loss of geometrical information about the cell of interest and the restriction of fluorescence intensity measurement to preselected spots or lines.

TABLE 1. SCHEMATIC OF THE QUAVIM SYSTEM

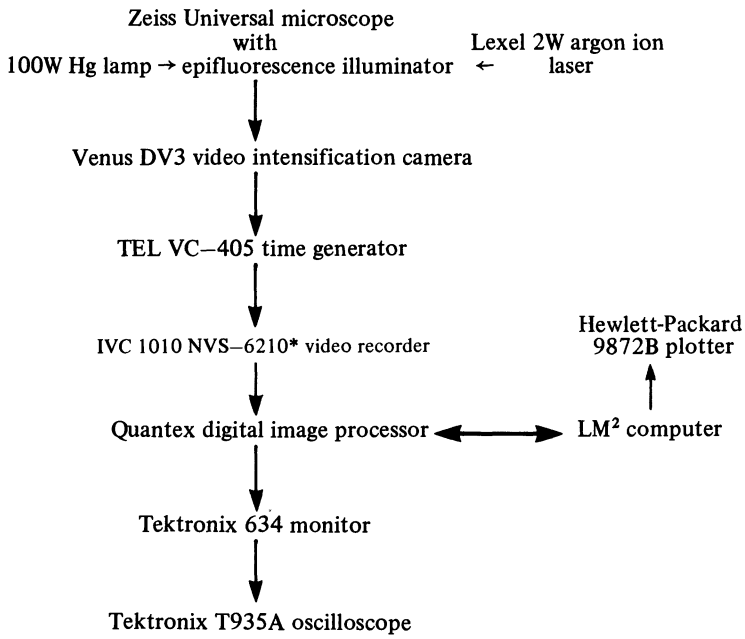

* JVC CR–6600 U, modified by National Video Services, Danbury, Connecticut, U.S.A.

We have therefore developed a second system based on high-resolution video recording and subsequent computer analysis of selected frames (quantitative video intensification microscopy, QUAVIM). A schematic description of the QUAVIM system is given in table 1. In brief, fluorescence-labelled cells are selected in an epifluorescence microscope by using a 100 W Hg (or 2 W argon-ion laser) light source, and fluorescence images are obtained by using a three-stage image intensification camera with vidicon tube and manual gain. This camera was selected for its superior resolution and decreased noise at low light levels compared with intensifiers with silicon-intensified target tubes. The image is routed via a time generator to a videotape recorder where raw (unprocessed) data are stored. For observation of the data during taping, recorder output is transferred via a Quantex Digital Image Processor to a high-resolution monitor. The signals from individual rasters are simultaneously displayed on an oscilloscope to check stability and absence of saturation. During taping, the image processor enables a variety of image manipulations (summation, averaging, image inversion, nonlinear display, etc.) that simply allows an improved view of the cell being investigated. However, its major role is in image analysis. The image processor is interfaced to a Logic Machine Minicomputer (LM^2), with 32 kbytes memory and magnetic tape storage. During tape playback selected, usually summed, frames are grabbed by the image processor and digitized by an 8 bit analogue–digital converter

PHILOSOPHICAL TRANSACTIONS OF THE ROYAL SOCIETY B BIOLOGICAL SCIENCES

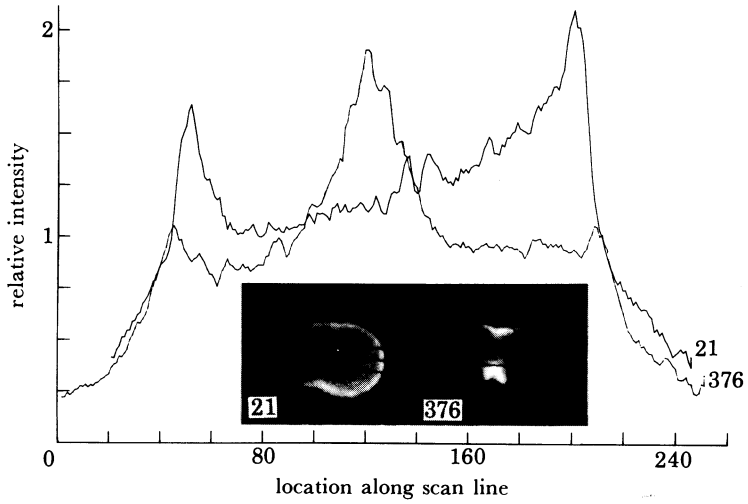

FIGURE 3. Typical QUAVIM scans of the summed F-Con A fluorescence across three lines spanning the long axis of a mitotic macrophage. The cell was labelled at 20 °C. Stage temperature was increased at 37 °C at 30 s. Summed (20 frames) images were selected in early anaphase (21 s) and late telophase (376 s). The photographs show the geometry of the cell at each point and the position of the scan lines.

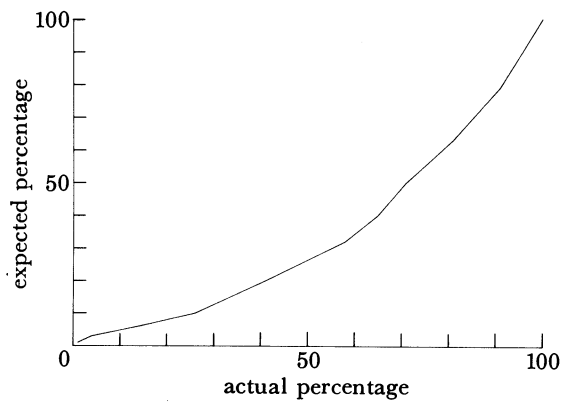

FIGURE 4. Linearization of fluorescence intensity measurements on the QUAVIM system. This typical plot of real to observed fluorescence was obtained by sequential attenuation with a graded series of neutral-density filters of the signal from a Zeiss fluorescence standard. This tape sequence is routinely generated at the end of each video recording.

into its large (512 × 512 × 12 bit) memory. The LM² can be used to select segments of the stored, digitized image for quantitative analysis. For example, figure 3 shows QUAVIM plots of fluorescence redistribution of Con A during cytokinesis. In this case three parallel lines were drawn through the central axis of the cell and the summed fluorescence intensities (minus background) at each of 240 locations along these lines were plotted as a function of time. The pattern of fluorescence loss at the poles and accumulation at the centre resembles the pattern obtained in the 26 point laser scan plot (figure 2). The accompanying Polaroid photographs taken from the c.r.t. screen show the exact location of these scans and the geometry of the entire cell.

QUAVIM data are corrected for the inherently nonlinear responses of the various video components, most notably the camera and tape recorders, by generation of a 'correction curve' at the end of each video sequence. A Zeiss fluorescence standard is mounted at the end of the

objective, focused onto the image intensifier and its fluorescence is recorded with all instrument settings unchanged. The standard is then recorded after insertion into the emission beam of a graded series of neutral-density filters ranging from 90 to 0.30% transmission. A plot of expected against actual fluorescence is obtained from the summed fluorescence across a line through this progressively attenuated image (figure 4) and is used to linearize the experimental data.

Since the coordinates of lines or areas to be analysed can be changed at will by selecting different parts of the stored image, the QUAVIM system can be used with moving cells, and

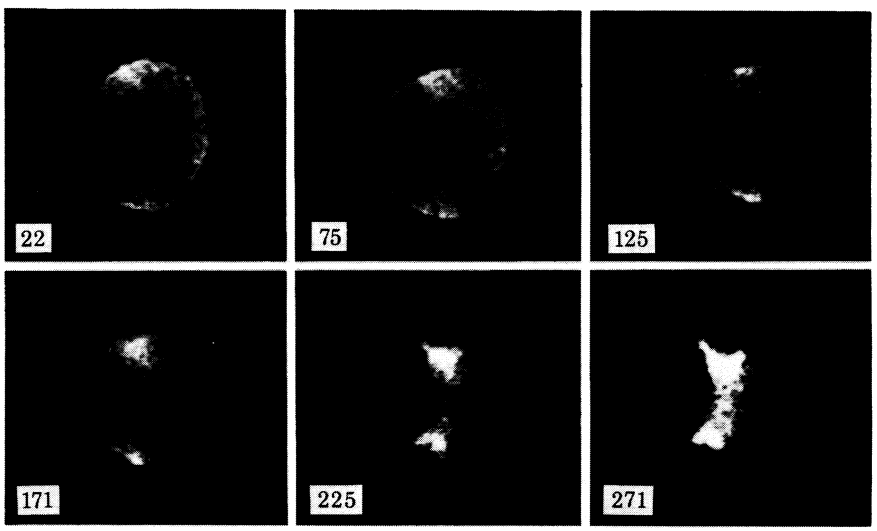

FIGURE 5. Frames from a video recording of a J774.2 macrophage labelled for 1 min at 37 °C with FS-Con A, selected for observation by epifluorescence illumination and viewed through an image intensification television camera. The distribution of fluorescence was recorded from metaphase through early G_1 by tape recording and subsequent transfer of selected processed (64 frame averaged) frames to a Tektronix 634 monitor for photography using Tri-X-Pan film in a Tektronix C-28 camera. Time is given in seconds.

recordings of the same cell can be analysed by a variety of methods. The QUAVIM system is, of course, suitable for measurement of molecular diffusion rates by laser illumination and FRAP analysis.

FS-CON A–RECEPTOR REDISTRIBUTION INTO THE CLEAVAGE FURROW

Figure 5 shows a few frames from a typical video recording of a FS-Con A-labelled J774.2 macrophage selected in metaphase and observed at 32 °C during the transition into anaphase and telophase. No asymmetry of fluorescence distribution is observed until the first appearance of the cleavage furrow, at which time there is simultaneous rapid redistribution of bound FS-Con A into the furrow. The redistribution here is complete in less than 3 min at 32 °C.

The rate of surface movement of the lectin was quantified by photon counting during a repetitive series of laser-excited fluorescence scans across the central axis of a series of similar FS-Con A-labelled cells selected in early anaphase and followed through telophase. Each scan took 10 s and monitored 26 predetermined points along a line across the long axis of the cell.

PHILOSOPHICAL TRANSACTIONS OF THE ROYAL SOCIETY B BIOLOGICAL SCIENCES

The resulting data were analysed in terms of two simple alternative models of lateral movement. In the first, the 'flow model', it was assumed that the net accumulation at the region of the developing cleavage furrow results from a directional flow of constant velocity, v, over the surface from the poles of the cell (assumed to be a sphere of radius r) to the centre. Random diffusion was taken to have a negligible effect. At the other extreme, the 'diffusion model' assumed that molecular motion occurs only by random diffusion on the surface of the sphere with diffusion coefficient D. In this case, we proposed that surface complexes that diffuse to the centre are immobilized and trapped.

The effective values of v and D were determined from measurements of the decrease with time of the mean-squared widths (or second moments, $\mu_2(t)$, about the mean along the scan axis) of the fluorescence distributions. This analysis has several advantages.

1. The second moments about the mean can be calculated simply and objectively according to the equation

$$\mu_2(t) = \frac{\sum_i x_i^2 F(x_i, t)}{\sum_i F(x_i, t)} - \left[\frac{\sum_i x_i F(x_i, t)}{\sum_i F(x_i, t)}\right]^2. \quad (1)$$

2. The second-moments calculation is particularly reliable since it weighs the extent of label depletion at the cell periphery, which is readily measured, and is relatively insensitive to the exact distribution of label at the furrow and to the changing cell geometry in this region.

3. Provided that a line scan is used to eliminate geometrical 'edge effects' that can distort the distribution of fluorescence intensity, then the second moment of the fluorescence distribution maintains a constant relation to the actual concentration of label at a given distance along the pole-to-pole axis.

4. V and D can be directly calculated either from the slope R_{max} of the plot of $\mu^2(t)$ with time ($R_{max} = -\frac{2}{3} vr$; $R_{max} = 0.47D$ according to the flow and diffusion models respectively) or from $\tau_{\frac{1}{2}}$, the half time of fluorescence loss from the poles ($\tau_{\frac{1}{2}} = 0.30\, r/v$; $\tau_{\frac{1}{2}} = 0.40 r^2/D$ according to the two models). The derivation of these relations is given in detail in Koppel *et al.* (1982).

Figure 6 presents the complete time course of $\mu_2(t)$ of three labelled cells followed through late anaphase and telophase. The cell radius was approximately 9 μm. The rates of receptor redistribution ($\pm$ standard deviations) calculated from the average value of R_{max} (-6.5×10^{-2} μm^2 s^{-1}) according to the 'flow' and 'diffusion' models respectively are $v = 0.7 \pm 0.2$ μm min^{-1} or $D = 1.4 \pm 0.5 \times 10^{-9}$ cm^2 s^{-1}. The rates calculated from the average value of $\tau_{\frac{1}{2}}$ (approx. 140 s) are respectively $v = 1.2 \pm 0.3$ μm min^{-1} and $D = 2.3 \pm 0.9 \times 10^{-9}$ cm^2 s^{-1}. In separate studies, the diffusion coefficients measured directly by FRAP on metaphase cells had an average value of 10^{-10} cm^2 s^{-1}. Thus a diffusion mechanism is not well supported by this result.

The results of subsequent FRAP measurements during the actual period of accumulation of Con A in the cleavage furrow definitely eliminated the diffusion mechanism. The fluorescence scan in figure 7 shows a relatively uniform distribution of FS-Con A on a cell selected at the onset of anaphase. A localized photobleaching pulse was used to decrease the concentration of intact fluorophore across one pole of this cell (the 'left side' in figures 7 and 8) to 50% of its initial level (figure 7*b*). During the first few minutes after photobleaching, the usual rapid transition to a marked central accumulation (figure 7*c*) was observed. The symbols in figure 8

PHILOSOPHICAL TRANSACTIONS OF THE ROYAL SOCIETY B BIOLOGICAL SCIENCES

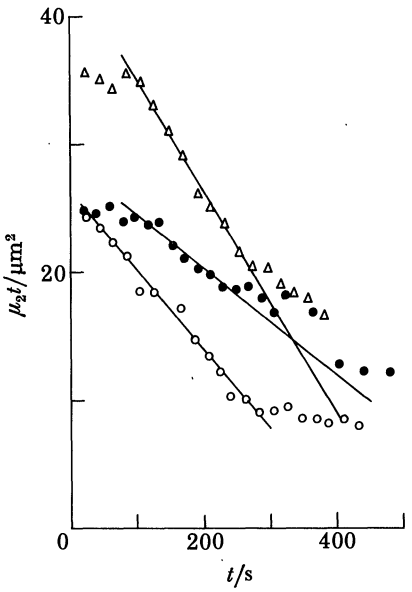

FIGURE 6. Time-course of calculated $\mu_2(t)$ for the distribution of F-S Con A fluorescence on three J774 macrophages followed through late anaphase and telophase. Slopes of straight lines superimposed on data were used in estimation of R_{max} values. $T = 37$ °C.

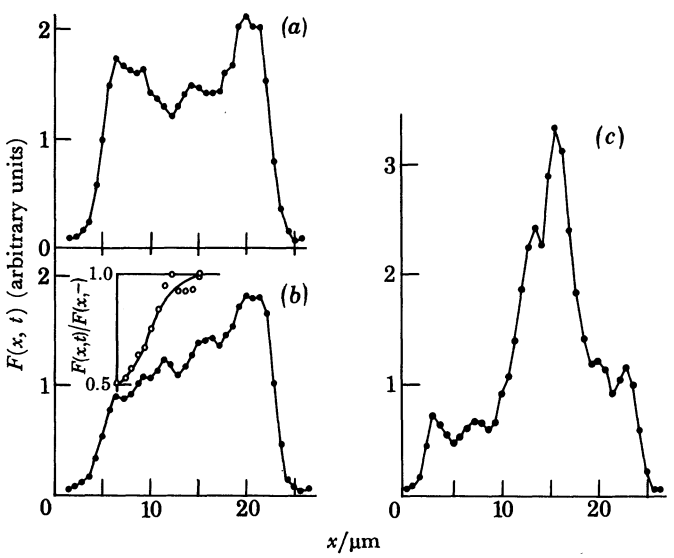

FIGURE 7. Scans of FS-Con A fluorescence on a mitotic J774 macrophage (*a*) in late anaphase before photobleaching ($t = 12$ s); (*b*) immediately after a photobleaching laser pulse directed at the edge of the scan profile ($t = 24$ s); and (*c*) subsequently in telophase ($t = 120$ s). Fluorescence scans were taken with the laser beam focused to a circularly symmetric spot, emphasizing the fluorescence at the cell edges and cleavage furrow. Bleaching was effected with a high-intensity laser beam defocused to a band across the cell, perpendicular to the scan axis. The inset to (*b*) shows the immediate post-bleach fluorescence distribution normalized by a pre-bleach scan.

show the measured intensities with time at the centre (furrow) and left and right edges of the same cell. These data points are superimposed on curves predicted for fluorescence redistribution by the diffusion (solid lines) or flow (broken lines) models. The flow model (broken lines) predicts no observable fluorescence recovery, i.e. back-diffusion at the bleached left edge. The diffusion model (solid lines) predicts an initial redistribution back into the bleached area. No

PHILOSOPHICAL TRANSACTIONS OF THE ROYAL SOCIETY B BIOLOGICAL SCIENCES

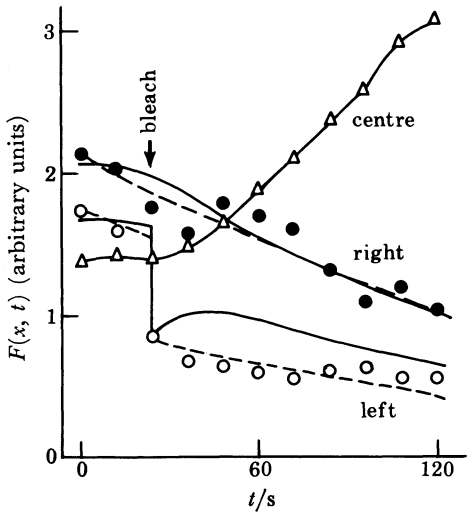

FIGURE 8. Time course of fluorescence intensity changes measured at the edges and central furrow on the cell of figure 7. Each value is the average of three or four adjacent data points from a complete high-resolution fluorescence scan. The solid and broken lines associated with the fluorescence data from the right (unbleached) and left (bleached) edges of the cell are theoretical curves derived for the diffusion and flow models respectively.

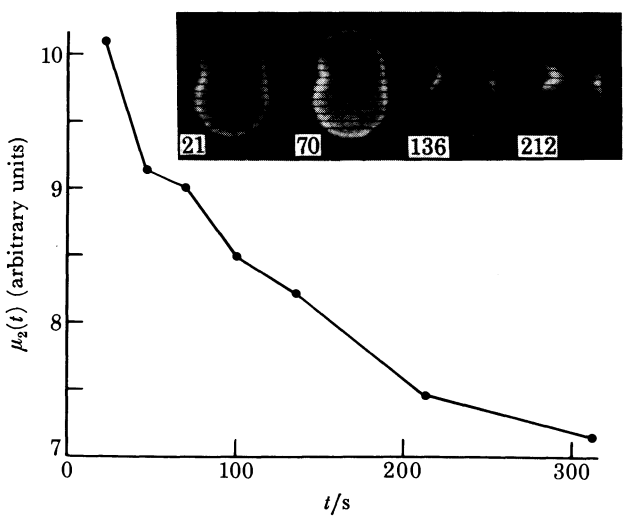

FIGURE 9. Time course of calculated $\mu_2(t)$ for the distribution of F-Con A fluorescence for a J774.2 macrophage followed from early anaphase to late telophase. Summed (15 frames) images were grabbed and digitized in the image processor. Fluorescence intensity readings were then taken across the series of equally spread parallel lines, seven above and seven below a line through the cleavage furrow. Second moments were calculated from the summed intensities across each line. The plot incorporates data from seven sequential frames. Photographs of distribution of fluorescence and location of the lines are shown for four of the seven frames.

recovery of fluorescence was measured at the bleached edge, indicating a unidirectional flow process.

We have used QUAVIM to reproduce the analysis of Con A redistribution into the cleavage furrow by the method of second moments. As shown in figure 9, an FS-Con A-labelled cell was video recorded during the transition from metaphase to anaphase. A series of summed frames were then selected for analysis as follows: fluorescence intensity readings were first taken from

PHILOSOPHICAL TRANSACTIONS OF THE ROYAL SOCIETY B BIOLOGICAL SCIENCES

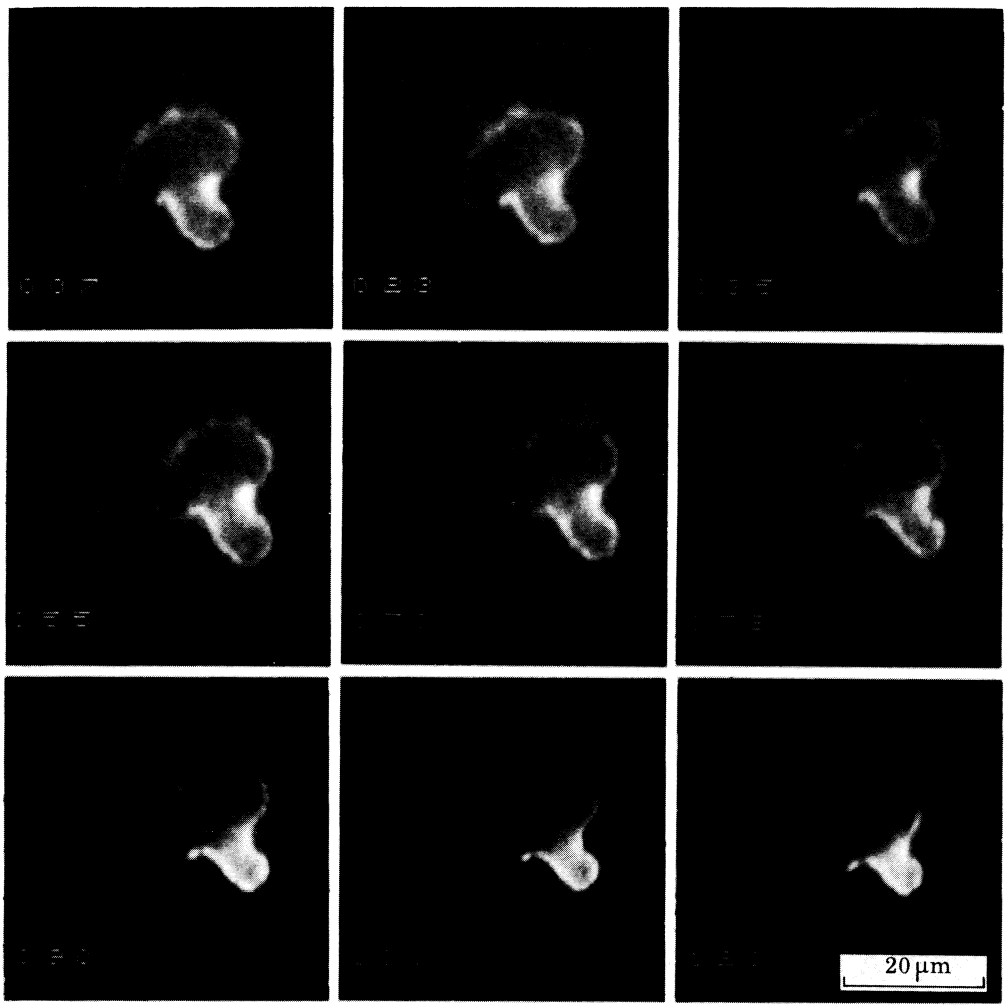

FIGURE 10. Frames photographed on Polaroid 611 film during playback of a processed (16 frame averaging) video recording of a protuberant J774.2 macrophage labelled for 30 s at 20 °C with FS-Con A then incubated at 37 °C on a microscope stage. Con A remains bound on the whole cell surface during approximately 0.5 min at 37 °C, then is redistributed abruptly from the cell body into the protuberance during a period of 10–20 s. Bar = 20 μm.

a series of seven equally spread parallel lines above and below a line through the furrow on each cell (see inset photographs). These readings were corrected for background fluorescence and nonlinearity and the second moments were then calculated according to (1) above. A rapid ($\tau_{\frac{1}{2}} \approx 120$ s) loss of fluorescence occurs from the poles. This value for $\tau_{\frac{1}{2}}$ and hence for v and D (where $r = 9$ μm) is in close agreement with the results obtained by laser scan analyses (above).

QUANTITATIVE ANALYSIS OF CON A–RECEPTOR MOVEMENT INTO CAP AND UROPOD MEMBRANES

As described above, ligand–receptor movement during capping and locomotion cannot readily be analysed by the laser scan technique owing to the simultaneous movement of both the whole cell and the ligand–receptor complexes that is incompatible with sequential record-

PHILOSOPHICAL TRANSACTIONS OF THE ROYAL SOCIETY B BIOLOGICAL SCIENCES

ings from the same points. We have thus depended on results obtained by QUAVIM to reveal the nature of the redistribution process during these two dynamic processes.

In the video sequence shown in figure 10, FS-Con A was bound more or less uniformly to the surface of a protuberant macrophage after brief (30 s) labelling at 20 °C. Upon warming to 37 °C, the distribution of fluorescence remained relatively unchanged for a further half

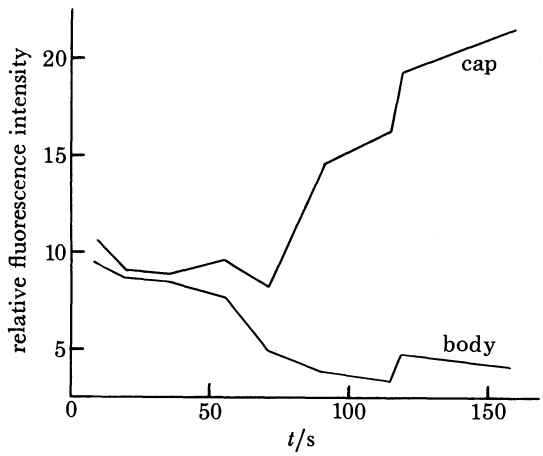

FIGURE 11. Change in fluorescence maxima at the cell body and cap with time. A series of five parallel lines were drawn through the midline of 15 summed images of the cell illustrated in figure 10. The maximum rate of fluorescence loss from the 'body' and increase in the 'cap' occurs over a period hardly exceeding 10 s. Since the cell was 20 μm long, an apparent diffusion constant of 10^{-8} cm^2 s^{-1} can be estimated from these data. Note that the greater apparent increase in fluorescence at the cap compared with its loss from the body reflects the geometry of the cell where fluorescence is concentrated from a large surface onto a smaller one.

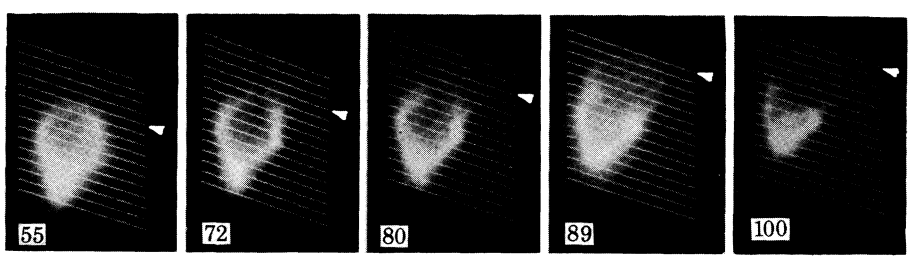

FIGURE 12. Frames photographed on Polaroid 611 film during playback of a processed (15 frame summation) video film of a F-Con A-labelled locomoting p.m.n. Cell monolayers were oriented by incubation at 37 °C for 15 min with 0.5 μM f-Met-Leu-Phe, then labelled at 10 °C for 30 s with 100 μg ml^{-1} F-Con A. A polarized cell was selected for observation at 10 °C and the stage temperature was increased to 25 °C at 45 s on this recording. A rapid clearing of fluorescence from the lamellipodium towards the uropod was observed. In this figure, a grid composed of 15 lines at 1.5 μm intervals is superimposed on each 15-summed frame by use of the LM^2 computer. Fluorescence intensity across each line was transferred to computer memory for further analysis. The arrowheads indicate the line across the lamellipodial tip (0 μm) for each frame. The total fluorescence intensity summed between lines 1 and 15 was essentially unchanged from frames 55 to 100, indicating relatively little loss of fluorescence due to bleaching, self-adsorption, saturation or other sources within this experiment (data not shown). Bar = 10 μm.

minute or so (to around 70 s on this recording). The Con A then moved rapidly to the surface overlying the protuberance.

The actual period of movement was determined by QUAVIM analysis of changes with time in the sum of the fluorescence intensities along a series of five parallel lines spanning the midline of the cell. Plots of the maximum fluorescence intensities of cell 'body' and cap (figure 11)

PHILOSOPHICAL TRANSACTIONS OF THE ROYAL SOCIETY B BIOLOGICAL SCIENCES

confirm that almost all of the FS-Con A is capped to the protuberance in a period of less than 20 s. The corresponding effective diffusion coefficient for this capping process on a cell 20 μm in diameter approaches 10^{-8} cm^2 s^{-1}. In this example, the estimated rate of ligand–receptor redistribution approaches diffusion rates measured for lipids and exceeds by 1 or 2 orders of magnitude the usual diffusion rates for proteins in biological membranes (Cherry 1979). FRAP analysis is thus not required here to distinguish diffusion from flow.

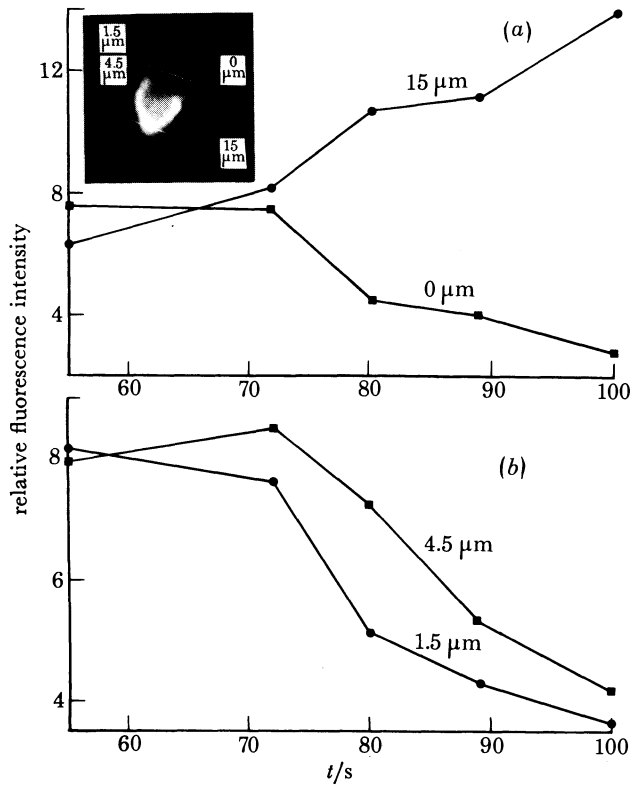

FIGURE 13. Summed fluorescence intensities with time of selected lines across a F-Con A-labelled, locomoting p.m.n. In (*a*), fluorescence intensity was summed across lines at 0 μm (lamellipodial tip) and 15 μm (uropod). In (*b*), fluorescence intensity was summed across lines at 1.5 μm and 4.5 μm behind the lamellipodium. The inset shows the position of these four lines at one time point (80 s).

A similar conclusion was drawn from studies of locomoting p.m.ns. In the video sequence shown in figure 12, fluorescein-conjugated Con A (F-Con A) was bound more or less uniformly to the surface of an f-Met-Leu-Phe treated human p.m.n. during 30 s of labelling at 10 °C. The temperature of the microscope stage was increased to 25 °C at 45 s on this recording. Warming was followed by an immediate contraction of the uropod and subsequent extension of the lamellipodium. F-Con A was displaced first from the lamellipodium and subsequently from the central section of the cell. Essentially all the F-Con A was in the uropod region by 100 s.

The grid of 15 parallel lines, 1.5 μm apart, drawn over these frames (figure 12) enabled the estimation of both the velocity of this F-Con A movement (backward) and cell movement (forward). First, since the grid is fixed in space, it may be calculated that the cell is displaced forward by approximately 6 μm in 45 s, or around 8 μm min^{-1}. More importantly, each line consists of approximately 80 locations across the cell, each with a characteristic fluorescence

intensity above background. Figure 13*a* shows the summed fluorescence intensities with time across equivalent lines running through the lamellipodial tip (0 μm) and through the midpoint of the uropod (15 μm). F-Con A is almost completely displaced from the lamellipodium between 70 and 80 s. It accumulates continuously at the uropod between 70 and 100 s. Figure 13*b* illustrates the summed fluorescence intensities with time across lines drawn 1.5 and 4.5 μm

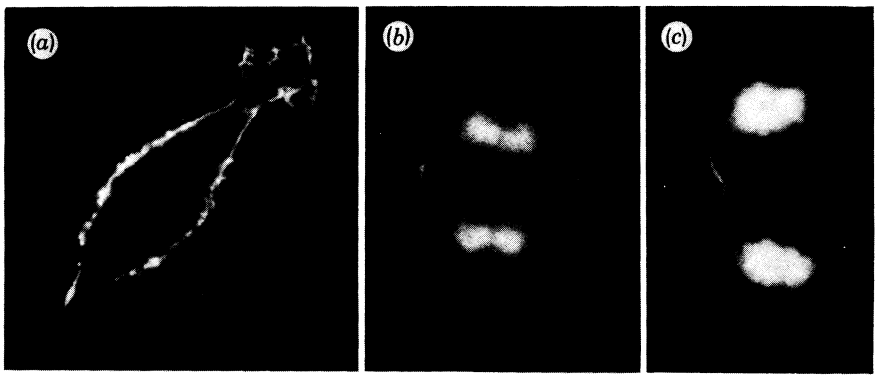

FIGURE 14. Distribution of F-CTB on J774.2 macrophages. Cell monolayers were incubated at 37 °C for 10 min with F-CTB, then fixed with 4% paraformaldehyde and incubated with Hoechst 33258, a DNA-binding dye that simplifies location of mitotic cells. The fluorescent ligand outlines the most delicate membrane folds and ruffles of the interphase cell (*a*). The regions of increased intensity most likely indicate regions of increased membrane accumulation. A remarkably uniform distribution of F-CTB fluorescence is seen at early anaphase before formation of the cleavage furrow (*b*). This essentially uniform labelling persists at late anaphase with only a hint of increased fluorescence intensity at the cleavage furrow (*c*).

from the lamellipodial tip. The loss of F-Con A–receptor complexes from the 1.5 μm line occurs at a maximum rate between 70 and 80 s. The loss of complexes from the 4.5 μm line occurs in parallel but is displaced in time by around 7 s. A similar displacement (not shown) was measured for the loss of F-Con A from the 7.5 μm line compared with the 4.5 μm line. Based on this displacement of approximately 7 s over a 3 μm distance, we calculate that F-Con A moved off the lamellipodium at about 26 μm min^{-1}. As in the capping experiment, an effective diffusion coefficient approaching 10^{-8} cm^2 s^{-1} would be required. Thus a mechanism of ligand–receptor redistribution based on diffusion seems unlikely. Similarly the hypothesis that ligand or particles may be simply left behind at the uropod as the cell moves forward (Schreiner & Unanue 1976; Wilkinson *et al.* 1980) is not well supported: the rate of movement of Con A–receptor complexes off the lamellipodium is at least three times faster than the rate of net forward cell locomotion. These data are thus most consistent with Con A–receptor redistribution by a process of directed migration.

THE TOPOGRAPHY OF OTHER MEMBRANE COMPONENTS AND MEMBRANE FUNCTIONS

So far, we have described in detail the ligand-induced redistribution of Con A receptors into cleavage furrow, cap, uropod and pseudopod membrane. We have shown that Con A receptors have an inherently uniform (or essentially so) distribution on cell surfaces. Their redistribution can be driven by both F-Con A and FS-Con A, indicating that extensive receptor cross-linking

PHILOSOPHICAL TRANSACTIONS OF THE ROYAL SOCIETY B BIOLOGICAL SCIENCES

by multivalent ligand is not essential to the redistribution process (of course it does not eliminate as essential a smaller degree of diffusion-dependent crosslinking).

In contrast with Con A receptors, fluorescein-conjugated choleratoxin B (F-CTB) maintains an apparently random distribution regardless of whether labelling is carried out at 4 °C or after fixation (to probe 'inherent' receptor topography) or at 37 °C (Koppel *et al.* 1982) This uniform binding of F-CTB presumably to GM1 ganglioside receptors on dividing cells is illustrated in figure 14. A similar uniform distribution of F-CTB is maintained on protuberant cells. We conclude that at least one membrane component can remain symmetrically distributed on asymmetric cells. Since the B-fragment is probably present as a pentamer, this distribution is maintained despite the probable occurrence of at least limited cross-linking of the ganglioside receptor.

In addition, some membrane components appear to be distributed away from cap and analogous regions. For example, the inherent distributions of Fc and C_3b receptors have been inferred from the binding of suitably opsonized particles or Ig aggregates at 4 °C or during incubation of less than 30 s at 37 °C. These receptors accumulate at the nuclear (non-protuberant) pole of colchicine-treated macrophages (figure 15*a*, plate 1) (Walter *et al.* 1980) and in the lamellipodial region of locomoting p.m.ns (Wilkinson *et al.* 1980; Walter *et al.* 1980). They can be redistributed to cap or uropod membrane by further 5 min incubation at 37 °C after the initial binding of opsonized particles (e.g. figure 15*b*). Transport carriers also appear to be excluded from membrane that accumulates ligand–receptor complexes. Tsan & Berlin (1971) reported that the activities of the membrane transport systems for adenine and lysine are completely unaltered after removal of up to 40% of the rabbit p.m.n. or alveolar macrophage surface by phagocytosis of latex. The most likely explanation was the segregation of transport carriers out of membrane that engulfs phagocytic particles and is internalized.

Remarkably, we have discovered that the development of membrane topographical asymmetry is not restricted to membrane receptors. A membrane macromolecular complex, the coated pit, is restricted to the same region that accumulates Con A–receptor complexes. This was first established by careful mapping of the distribution of coated pits in colchicine-treated protuberant macrophages (Pfeiffer *et al.* 1980): as shown in figure 16, plate 1, coated pits are exclusively localized to the protuberance. Subsequently, Davis *et al.* (1982) documented their restriction to the uropod of locomoting p.m.ns (figure 17, plate 2). In addition, Aggeler & Heuser (1981) have established that the pseudopod membrane of phagocytizing macrophages is also enclosed by coated membrane. In contrast, pits are essentially distributed at random on symmetrical cells (actually as random clusters in the case of resting J774.2 macrophages) (Pfeiffer *et al.* 1980).

Accompanying this strict segregation of coated pits, the uptake by fluid pinocytosis of fluorescein–dextran as well as the uptake by adsorptive pinocytosis of F-Con A is confined to the protuberance of colchicine-treated macrophages (figure 18, plate 2) (Walter *et al.* 1980) and the uropod of locomoting p.m.ns (Davis *et al.* 1982). All endocytic processes are completely arrested in mitosis from the onset of prophase to telophase (Berlin *et al.* 1978; Berlin & Oliver 1980). The recovery of pinocytic activity at the onset of G_1 is first observed in the region of the cleavage furrow.

These various topographical data are summarized in table 2. Their essence is the variability of receptor topography and the extension of membrane topographical asymmetry on polarized cells beyond membrane receptors to membrane macromolecular complexes and endocytic

PHILOSOPHICAL TRANSACTIONS OF THE ROYAL SOCIETY B BIOLOGICAL SCIENCES

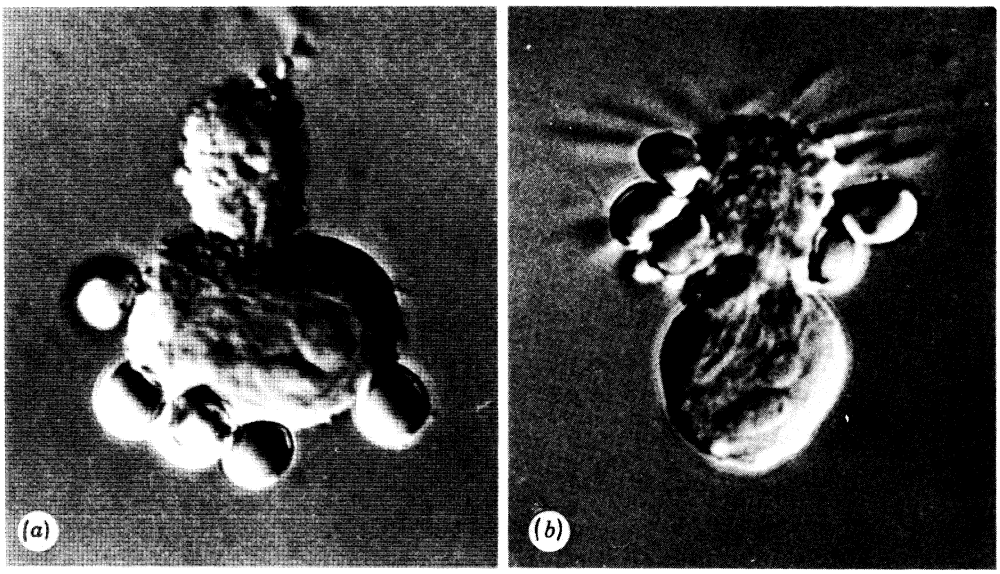

FIGURE 15. The distribution of complement-opsonized erythrocytes on colchicine-treated macrophages. After 45 s at 37 °C, erythrocytes are bound at the nuclear pole of the cell (*a*). They redistribute to the protuberance after rinsing and further incubation for 5 min or more at 37 °C (*b*).

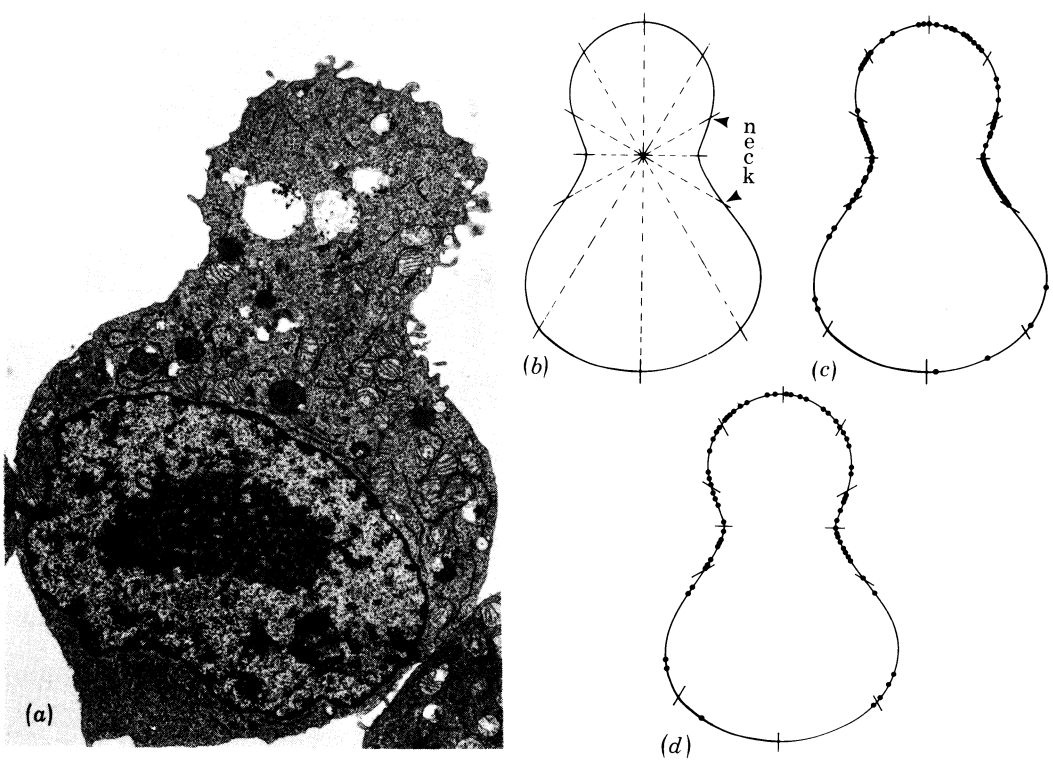

FIGURE 16. The distribution of coated pits on protuberant cells. A cumulative map of coated pit topography was built by translocating pits from individual electron micrographs (*a*) onto equivalent quadrats (equal-length segments along the surface profile) of a diagrammatic cell (*b*) whose dimensions were proportional to those of the original cell. The results of two typical experiments, each analysing 12 randomly chosen protuberant J774.2 macrophages from colchicine-treated (10 μm, 60 min) populations, are given in (*c*) and (*d*). They demonstrate the concentration of pits in the 'neck' and 'head' regions of protuberant cells.

(*Facing p.* 228)

PHILOSOPHICAL TRANSACTIONS OF THE ROYAL SOCIETY B BIOLOGICAL SCIENCES

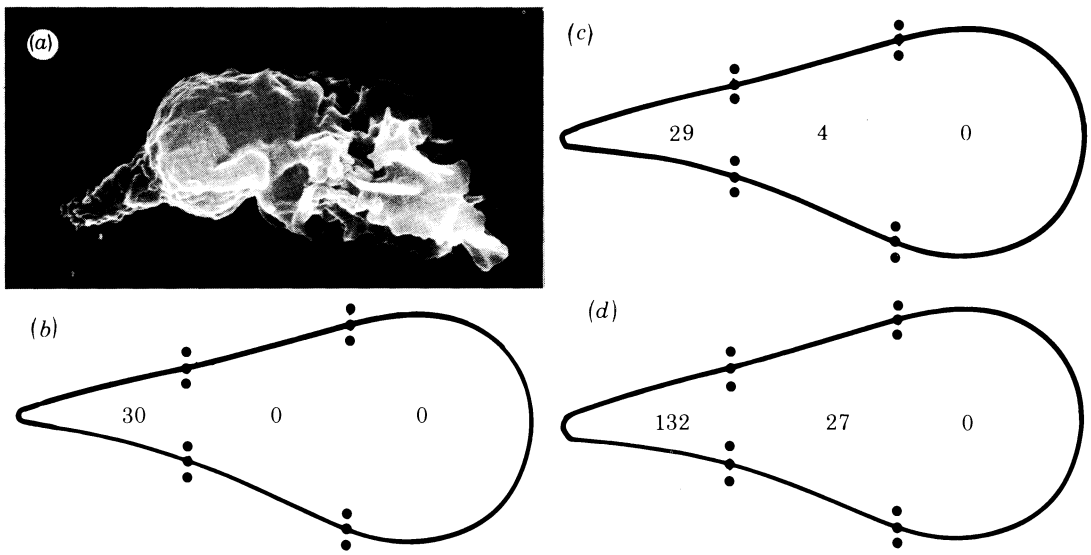

FIGURE 17. The topography of coated pits and coated vesicles during chemotaxis in human p.m.ns. The numbers of coated pits (*b*, *c*) or pits and coated vesicles (*d*) occupying the anterior, central or posterior thirds of the total cell perimeter were determined in human p.m.ns polarized by 20 min incubation in a gradient (*a*, *c*) or in suspension (*b*) with f-Met-Leu-Phe (0.1 μM). The results in (*b*) were obtained by analysis of 10 cells from two separate experiments; (*c*) is from 16 cells from two experiments; and (*d*) analyses 17 cells from three experiments; (*a*) illustrates the typical polarized morphology of locomoting p.m.ns. (S.e.m.; magn. ×4500.)

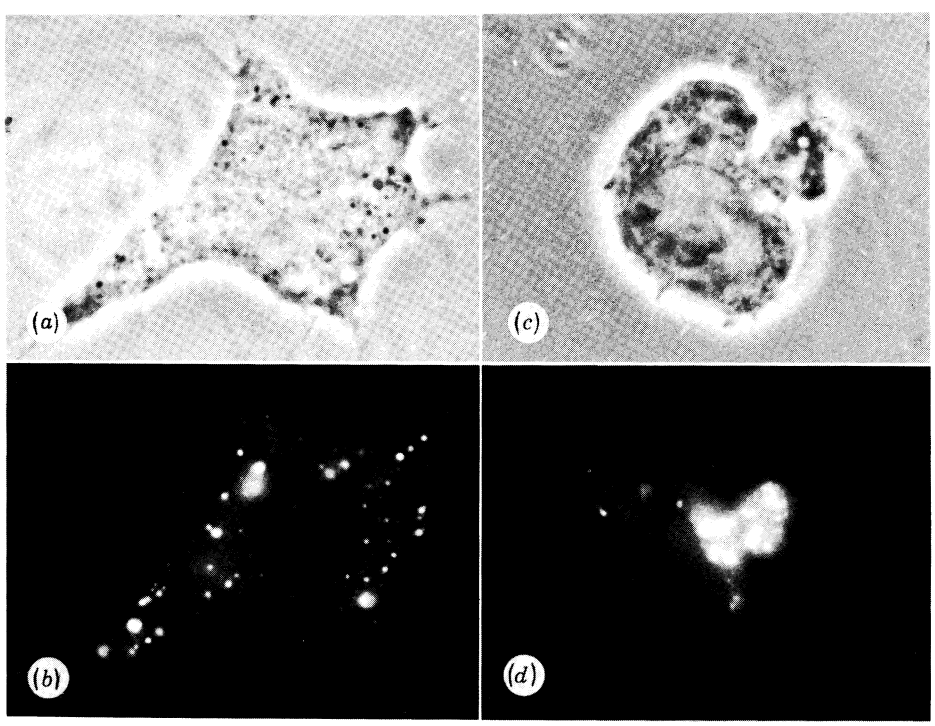

FIGURE 18. The topographical restriction of pinocytosis in protuberant macrophages. The untreated, spread macrophage ingests fluorescein-dextran by fluid pinocytosis from points over the whole surface (*a*, *b*). In contrast, fluorescein-dextran uptake is confined to the protuberance of the colchicine-treated cell. Both cells were incubated at 37 °C for 5 min with 5 mg ml^{-1} fluorescein-dextran.

PHILOSOPHICAL TRANSACTIONS OF THE ROYAL SOCIETY B BIOLOGICAL SCIENCES

functions. Most importantly, the analogy between cap, pseudopod, uropod and cleavage furrow membranes holds for every receptor or function tested so far.

TABLE 2. PATTERNS OF MEMBRANE ASYMMETRY ON POLARIZED CELLS

(This table lists membrane probes studied in our laboratory. In most cases the same asymmetry is produced whether analysis is performed with protuberant, oriented, phagocytizing or dividing cells. However not all probes have been studied under all four conditions. List C, in particular, can be greatly expanded by reference to the literature on membrane capping.)

A. *components and functions that remain partly or fully dispersed on polarized cells*
Con A receptors
gangliosides

B. *components and functions that segregate away from protuberance, uropod, pseudopod and/or cleavage furrow membranes*
transport carriers
Fc receptors
C3b receptors

C. *components and functions concentrated in protuberance, uropod, pseudopod and/or cleavage furrow membranes*
Con A–receptor complexes
Fc–receptor complexes
C3b–receptor complexes
fluid pinocytosis
adsorptive pinocytosis
phagocytosis
coated pits

MECHANISMS CONTROLLING RECEPTOR TOPOGRAPHY: MODELS BASED ON MICROFILAMENT–RECEPTOR INTERACTION

If diffusion is not the basic process underlying long-range surface movements of ligand–receptor complexes, what can be said of the unidirectional mechanism? Clearly some force is applied to the membrane, which imparts movement to the ligand–receptor complex. Since capping processes are blocked by cytochalasins, many investigators have concluded that these forces are generated by direct or indirect interactions of membrane-linked microfilaments with receptors (see, for example, Edelman *et al.* 1973; Edelman 1976; DePetris 1976; Schreiner & Unanue 1976; Bourguignon & Singer 1977).

Consistent with the various forms of this familiar hypothesis, our comparative studies by electron microscopy and specific anti-actin immunofluorescence have consistently emphasized the exclusion of cytoplasmic organelles and the concentration of cortical microfilaments underlying cap, pseudopod, cleavage furrow and uropod membranes (Albertini *et al.* 1976; Berlin & Oliver 1978; Oliver *et al.* 1976, 1977; Oliver & Berlin 1979, 1982; Koppel *et al.* 1982; Davis *et al.* 1982). This hypothesis is also consistent with recent evidence for ligand-induced linkage of both receptors and actin to detergent-extracted 'cytoskeletons' of various cell types (see, for example, Sheterline & Hopkins 1981).

However, we have emphasized that the concentration of microfilaments may be present *before* the accumulation of ligand–receptor complexes (see figures 10 and 12, where Con A–receptor complexes migrate onto an existing protuberance and uropod respectively). Thus the microfilament aggregation is not the result of movement, nor does receptor accumulation necessarily occur *pari passu*. We have also emphasized that not all regions of microfilament concentration are regions of ligand–receptor accumulation: for example, the anterior lamellipodia of moving neutrophils are supported by a dense meshwork of microfilaments (see, for example, Davis *et al.* 1982) but ligand–receptor complexes redistribute to the posterior or uropod region (figure 12). Furthermore, other investigators have reported the ability of antibodies to simulate capping of a range of endogenous and introduced surface determinants that

PHILOSOPHICAL TRANSACTIONS OF THE ROYAL SOCIETY B BIOLOGICAL SCIENCES

specifically should not interact with submembranous microfilaments. These include Forssman antigen, a membrane glycolipid (Stern & Bretscher 1979); *N*-2,4,6-trinitrophenyl-1-acyl-2-(*N*-4-nitrobenzo-2-oxa-1,3-diazole) aminocaproyl phosphatidylethanolamine, a fluorescent phospholipid analogue (Schroit & Pagano 1981); and stearoyldextran, an impermeable fatty acid analogue (Wolf *et al.* 1980). Finally, recent studies by Koppel and colleagues (Sheetz *et al.* 1980; Koppel *et al.* 1981) in spherocytic mouse erythrocytes that lack the principal components of the erythrocyte cytoskeletal matrix (normally consisting of spectrin, actin and bands 4.1 and 4.9) have established that the diffusion coefficient of the major membrane proteins in the mutant red cells ($2.5 \pm 0.6 \times 10^{-9}$ cm^2 s^{-1}) is two orders of magnitude greater than that measured in normal cells ($4.5 \pm 0.8 \times 10^{-11}$ cm^2 s^{-1}). This raises the possibility that microfilament–membrane interaction may actually *impair*, not promote, the mobility of membrane components.

Of course, most cells probably have an excess of actin. Hence even if most filaments are organized away from a particular receptor, the possibility remains that it can still link to an available filament after ligand binding and thus be swept to the region of larger accumulation. As pointed out by Oliver & Berlin (1982) there is a persistent thin network of submembranous microfilaments away from the regions of microfilament enrichment. However, Loor (1976) has emphasized that the dimension of the microfilaments (5–7 nm) precludes their packing at the surface density of many receptors. Further, even if filament–receptor complexes are mobile, it follows that the new filament–receptor complex must be swept through a mat of unattached microfilaments. No evidence for lability of this magnitude in actin gels is available.

Based on these diverse arguments, we conclude that ligand-induced interactions of receptors with microfilaments may occur *after* receptor redistribution and may indeed be essential for the endocytosis of ligand–receptor complexes. The redistribution process itself may not be immediately dependent on the interactions of receptors with microfilaments. We have thus considered alternative models in which certain accumulations of actin filaments could cause directional movement at a distance.

Mechanisms controlling receptor topography: models based on directional flow of membrane lipid or whole membrane

Bretscher (1976) and Harris (1976) have both postulated flow models that could accommodate unidirectional receptor migration independent of direct microfilament–receptor interaction. In these models membrane lipid (Bretscher) or whole membrane (Harris) is postulated to flow continuously from the front of the cell to the rear where it is removed by dissolution or endocytosis and recycled to the front. According to Bretscher's model, ligand–receptor complexes are swept along with the lipids, whereas unoccupied receptors escape by back-diffusion. Harris's model involves movement of all membrane components. In both models, a molecular filter excludes ligand–receptor complexes from internalization and recycling. The net result is cap formation at the site of filtration.

This model relieves cytoplasmic microfilaments of an obligatory direct role in topographical control. However, neither the force for this directed flow of membrane nor the nature of the filter is defined; the postulated exclusion of ligand–receptor complexes from the cytoplasmic milieu is inconsistent with the observation that complexes are in fact rapidly internalized from regions of cap formation; and we see no evidence for insertion of vesicles into the membrane

PHILOSOPHICAL TRANSACTIONS OF THE ROYAL SOCIETY B BIOLOGICAL SCIENCES

opposite regions of ligand–receptor accumulation (the insertion of dissolved or micellar membrane components is still possible). Our evidence that ligand–receptor complexes migrate to the cleavage furrow of anaphase cells, although endocytosis is arrested until G_1, seems inconsistent with a membrane flow model linked to continuous membrane internalization and recycling. Similarly, the intermittent course of lectin–receptor redistribution, apparent in the capping sequence (figure 4) would not be predicted by these models. Finally, FRAP analyses have shown that the diffusion coefficient of proteins in biological membranes is consistently low, and that a substantial portion of most membrane proteins is effectively immobile, i.e. cannot diffuse into a bleached region. In contrast, FRAP measurements confirm that lipid diffuses extremely rapidly (Cherry 1979). These widely accepted results present problems for both flow models. Harris's model would predict the fairly rapid anisotropic recovery of fluorescence due to migration of unbleached proteins into and past a bleached region. Immobile membrane components are not predicted. Bretscher's model proposes the flow of lipid past back-diffusing proteins. However, even if lipid were added continuously to the membrane and removed at the opposite pole, causing a flow of membrane, one would still expect to favour the randomization of lipid and the movement of protein, not vice versa.

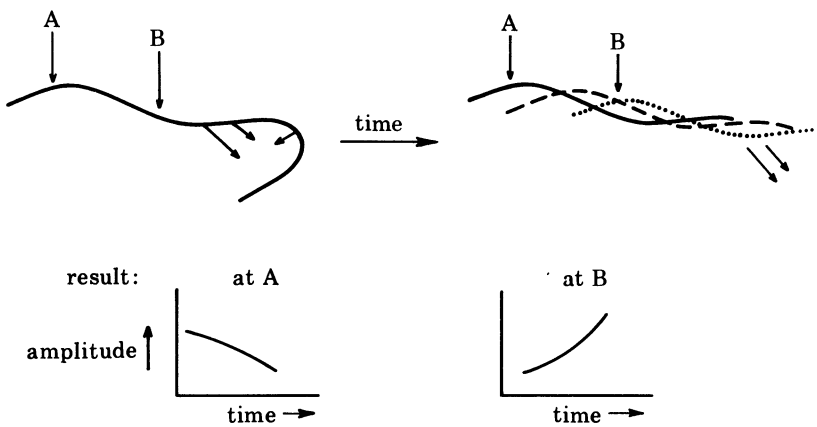

FIGURE 19. A model for the generation of oriented waves in cell surfaces. Tension acting inward and along the membrane (arrows) provides force for the progressive displacement of the membrane. The resulting oscillation of amplitude with time at any chosen point on the membrane constitutes a wave oriented towards the region of force generation.

MECHANISMS CONTROLLING RECEPTOR TOPOGRAPHY: SURFBOARDING

Oliver & Berlin (1982) have proposed an alternative model in which wave motion provides the force for the selective movement of surface constituents by a process resembling surfboarding. The model is drawn from the experimental data developed above and from the theoretical work of Hewitt (1979).

The model postulates the generation of waves moving across the surface of polarized cells. It is proposed that the formation of a uropod, pseudopod or analogous structure by local recruitment of microfilaments to the membrane generates tension directed inward and along the membrane. This asymmetric application of tension in turn initiates membrane movements perpendicular to the surface with the peak and crest displaced laterally with time, i.e. mechanical waves (figure 19). The precise point of origin and the orientation of these waves is determined by the

PHILOSOPHICAL TRANSACTIONS OF THE ROYAL SOCIETY B BIOLOGICAL SCIENCES

relation of the regions of tension to cell geometry. The narrow band of microfilaments that underlies the entire cell periphery may play a role in the transmission of this tension.

For transverse waves, matter moves or oscillates at right angles to the direction of wave motion. Thus once oriented wave motion is initiated, most membrane components behave essentially as corks on water: as the wave passes they oscillate between wave trough and wave crest, undergoing changes in orientation but little net movement. However, selected membrane constituents are transported in the direction of wave motion. This occurs if the constituent develops an energetically favourable interaction with a point on the wave surface corresponding to a particular phase of the wave motion (figure 20). For example, a membrane component may 'fit' ideally to the geometry of a wave peak. To displace the constituent from this point

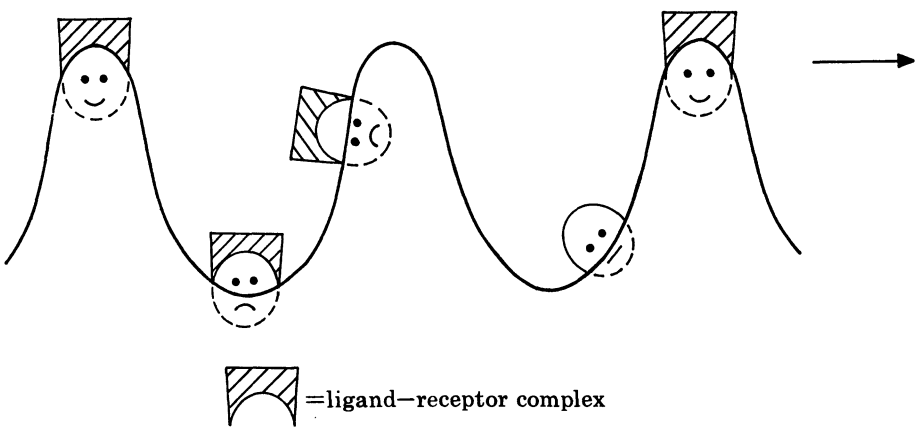

FIGURE 20. Response of membrane determinants to the passage of waves. Certain receptors sense a change in orientation but no large change in environment as the waves progress. These occupy random positions on the cell surface. Other receptors and ligand–receptor complexes are preferentially associated with particular regions of the waves (the crests in this diagram) and retain this distribution. These move with the waves to the region of force generation.

now requires energy. Transport is favoured if the energy for displacement is greater than that required to transport the constituent along the wave at an equivalent point of the wave surface. This is essentially how surfboards operate. The shape of the surfboard interacts favourably along the wave crest. As the crest is displaced the board will tend to move along with it. (With surfboards, gravity of course eventually provides an even greater energy trough.) Constituents entrained in waves may be 'beached' by the termination of the wave at the protuberance, uropod, pseudopod, cleavage furrow or equivalent region (and may subsequently be internalized by endocytosis, which we have shown is largely restricted to these regions).

According to Hewitt, entrainment on these waves will depend in large part on the relation of the ligand–receptor complex to wave geometry. However, for a component localized within a membrane, various additional factors may modulate entrainment by increasing the energy required for translocation. In particular, entrainment may be impaired by drag due to the viscosity of the lipid bilayer, to interactions with other membrane components and to interaction of cytoskeletal elements with the membrane bilayer. It may, on the other hand, be promoted by the local reorganization of membrane lipids (or protein, or both) along the wave membrane. For example, Lentz *et al.* (1976) have reported lipid phase separations associated with changes in the radius of membrane curvature: positive interaction of a particular receptor

PHILOSOPHICAL TRANSACTIONS OF THE ROYAL SOCIETY B BIOLOGICAL SCIENCES

or ligand–receptor complex with such a locally reconstructed membrane could promote entrainment.

Our model seems to accommodate a variety of observations that do not readily fit other models. It provides a mechanism for local membrane–microfilament interactions to influence the distribution of receptors located at a distance. It predicts the rapid, unidirectional redistribution of ligand–receptor complexes as reported here for Con A–receptor complexes: once a membrane determinant is entrained by a wave, its motion is no longer determined by its intrinsic diffusion rate but is primarily a function of the speed and orientation of the wave. It also predicts that in general, because of geometrical and other considerations discussed below, larger membrane determinants will move with the waves whereas the distribution of many smaller components may be unaffected. Consistent with this, coated pits, which constitute macromolecular aggregates, accumulate at protuberance and uropod membranes. The model can explain the delay followed by abrupt redistribution of ligand–receptor complexes observed in the capping sequence (figure 10) and the existence of a lag between successive clearings of surface complexes. It readily accommodates the capping of probes that insert only part way through the membrane bilayer and so cannot interact directly with cytoskeletal structures.

The hypothesis can be applied to explain the short-range membrane asymmetries of relatively unperturbed cells. For example an interphase macrophage incubated in suspension maintains a more or less rounded shape (Walter *et al.* 1980) organizes its coated pits in a random array of small clusters (Pfeiffer *et al.* 1980); performs pinocytosis over the whole surface (figure 18) and redistributes bound ligands such as Con A into randomly distributed patches that are subsequently ingested (Walter *et al.* 1980). We think it likely that the processes of microfilament recruitment and wave generation occur intermittently in local regions over the whole membrane of such relatively symmetrical cells, producing multiple randomly oriented waves over the cell surface. These waves would lead to surface patching of ligand–receptor complexes and to the clustering of coated pits. However, interference between interacting waves would prevent their support of long-range movements.

During mitosis, no patching or capping of ligand–receptor complexes occurs and endocytosis is completely arrested (Berlin *et al.* 1978; Berlin & Oliver 1981). We suppose that these properties reflect the relative loss of even short-range wave motion in mitotic cells.

Inferential evidence for the existence of wave-like movement on the cell surface is abundant. Ramsey (1972), Senda *et al.* (1975, 1979), Englander (1980) and Keller & Cottier (1981) have all described the continuous posterior movement of membrane folds and plications from the anterior tip of the lamellipodium towards the constricting ring on migrating neutrophils and on neutrophils oriented in suspension by incubation with chemotactic factors. The constricting ring in turn flows backward in a wave-like motion as the cell advances. Estimates of the time required for complete passage of this 'contraction wave' from lamellipodium to uropod vary from 1–3 min (Senda *et al.* 1979) to less than 1 min (Keller & Cottier 1981). Trinkaus (1980) has described similar protrusive activity at the lamellipodium of a variety of tissue cells with constant generation and backflow of extensively plicated membrane. This protrusive activity and wave-like propagated movement backwards of plicated membrane is increased after colchicine treatment. According to Chen (1979), protrusive activity may occur intermittently. Further, it can be abruptly increased by retraction of membrane at another region (usually the opposite pole) of the cell. This compensatory withdrawal of membrane at one site to allow protrusive activity elsewhere may enable cells to maintain directional movement without con-

PHILOSOPHICAL TRANSACTIONS OF THE ROYAL SOCIETY B BIOLOGICAL SCIENCES

tinuous insertion of new membrane at the leading front. Abercrombie, Harris and others have described in detail the flow of attached particles and ligand (beads, Con A–receptor complexes) in association with the flow of plicated membrane on moving (adherent) fibroblasts (reviewed by Harris 1973).

Experiments are now in progress to correlate membrane geometry with the wavelike movement of ligand–receptor complexes. These studies may reveal the mechanism(s) of wave production and of the entrainment of selected receptors on waves.

This work was supported in part by N.I.H. grant no. CA-15544 and by grant no. BC-179 from the American Cancer Society. J.M.O. holds an A.C.S. Faculty Research Award.

References

Aggeler, J. & Heuser, J. G. 1980 Phagocytosis visualized at high resolution from inside and outside the cell. *J. Cell Biol.* **87**, 93a.

Albertini, D. F., Berlin, R. D. & Oliver, J. M. 1977 The mechanism of Concanavalin A cap formation in leukocytes. *J. Cell Sci.* **26**, 57–75.

Berlin, R. D. & Oliver, J. M. 1978 Analogous ultrastructure and surface properties during capping and phagocytosis in leukocytes. *J. Cell Biol.* **77**, 789–804.

Berlin, R. D. & Oliver, J. M. 1980 Surface functions during mitosis. II. Quantitation of pinocytosis and kinetic characterization of the mitotic cycle using a new fluorescence technique. *J. Cell. Biol.* **85**, 660–671.

Berlin, R. D. & Oliver, J. M. 1982 The movement of bound ligands on cell surfaces. *J. theor. Biol.* (In the press.)

Berlin, R. D., Oliver, J. M. & Walter, R. J. 1978 Surface functions during mitosis. I. Phagocytosis, pinocytosis and mobility of surface-bound Con A. *Cell* **15**, 327–341.

Bourguignon, L. Y. W. & Singer, S. J. 1977 Transmembrane interactions and the mechanism of capping of surface receptors by their specific ligands. *Proc. natn. Acad. Sci. U.S.A.* **74**, 5031–5035.

Bretscher, M. S. 1976 Directed lipid flow in cell membranes. *Nature, Lond.* **260**, 21–23.

Chen, W.-T. 1979 Induction of spreading during fibroblast movement. *J. Cell. Biol.* **81**, 584–691.

Cherry, R. J. 1979 Rotational and lateral diffusion of membrane proteins. *Biochim. biophys. Acta* **559**, 289–307.

Davis, B. H., Walter, R. J., Pearson, C. B., Becker, E. L. & Oliver, J. M. 1982 Membrane activity and topography of f-Met-Leu-Phe-treated polymorphonuclear leukocytes: acute and sustained responses to chemotactic peptides. *Am. J. Path.* **108**, 206.

DePetris, S. 1977 Distribution and mobility of plasma membrane components on lymphocytes. In *Dynamic aspects of cell surface organization* (ed. G. Poste & G. L. Nicolson), pp. 644–728. New York: Elsevier/North-Holland.

Edelman, G. M. 1976 Surface modulation in cell recognition and cell growth. *Science, Wash.* **192**, 218–226.

Edelman, G. M., Yahara, I. & Wang, J. L. 1973 Receptor mobility and receptor-cytoplasmic interactions in lymphocytes. *Proc. natn. Acad. Sci. U.S.A.* **70**, 1442–1446.

Englander, L. L. 1980 Human leukocyte locomotion: cytoplasmic flow and contacts with the substratum. *J. Cell Biol.* **87**, 89a.

Harris, A. K. 1973 Cell surface movements related to cell locomotion. In *Locomotion of tissue cells* (*Ciba Foundation Symposium* no. 14), pp. 3–26.

Harris, A. K. 1976 Recycling of dissolved plasma membrane components as an explanation of the capping phenomenon. *Nature, Lond.* **263**, 781–783.

Hewitt, J. A. 1979 Surf-riding model for cell capping. *J. theor. Biol.* **80**, 115–127.

Keller, H. U. & Cottier, H. 1981 Crawling like movements and polarization in non-adherent leukocytes. *Cell. Biol. int. Reps* **5**, 3–7.

Koppel, D. E. 1979 Fluorescence redistribution after photobleaching. A new multipoint analysis of membrane translational dynamics. *Biophys. J.* **28**, 281–291.

Koppel, D. E., Oliver, J. M. & Berlin, R. D. 1982 Surface functions during mitosis. III. Quantitative analysis of ligand–receptor movement into the cleavage furrow: diffusion vs flow. *J. Cell Biol.* **93**, 950–960.

Koppel, D. E., Sheetz, M. P. & Schindler, M. 1981 Matrix control of protein diffusion in biological membranes. *Proc. natn. Acad. Sci. U.S.A.* **78**, 3576–3581.

Lentz, B. P., Barenholz, Y. & Thompson, T. E. 1976 Fluorescence depolarization studies of phase transitions and fluidity in phospholipid bilayers. 2. Two-component phosphatidylcholine liposomes. *Biochemistry, Wash.* **15**, 4529–4537.

Loor, F. 1976 Cell surface design. *Nature, Lond.* **264**, 272–273.

PHILOSOPHICAL TRANSACTIONS OF THE ROYAL SOCIETY B BIOLOGICAL SCIENCES

Oliver, J. M. & Berlin, R. D. 1979 Microtubules, microfilaments and the regulation of membrane functions. *Symp. Soc. exp. Biol.* **33**, 277–298.
Oliver, J. M. & Berlin, R. D. 1982 Mechanisms that regulate the structural and functional architecture of cell surfaces. *Int. Rev. Cytol.* **74**, 55–94.
Oliver, J. M., Krawiec, J. A. & Becker, E. L. 1978 The distribution of actin during chemotaxis in rabbit neutrophils. *J. reticuloendothel. Soc.* **24**, 697–704.
Oliver, J. M., Lalchandani, R. & Becker, E. L. 1977 Actin redistribution during Concanavalin A cap formation in rabbit neutrophils. *J. Reticuloendothel. Soc.* **21**, 357–364.
Pfeiffer, J. R., Oliver, J. M. & Berlin, R. D. 1980 Surface topography of coated pits. *Nature, Lond.* **286**, 727–729.
Ramsey, W. S. 1972 Locomotion of human polymorphonuclear leukocytes. *Expl Cell Res.* **72**, 489–501.
Schreiner, G. F. & Unanue, E. R. 1976 Membrane and cytoplasmic changes in B lymphocytes induced by ligand-surface immunoglobulin interaction. *Adv. Immunol.* **24**, 38–165.
Schroit, A. J. & Pagano, R. E. 1981 Capping of a phospholipid analog in the plasma membrane of lymphocytes. *Cell* **23**, 105–112.
Senda, N., Shibata, N., Tamura, H. & Yoshitake, J. 1979 Leukocytic movement and contractile protein. *Meth. Achiev. exp. Path.* **9**, 169–186.
Senda, N., Tamura, H., Shibata, N., Yoshitake, J., Kondo, K. & Tanaka, K. 1975 The mechanism of the movement of leukocytes. *Expl Cell Res.* **91**, 393–407.
Schindler, M., Osborne, M. J. & Koppel, D. E. 1980 Lateral mobility in reconstituted membranes – comparisons with diffusion in polymers. *Nature, Lond.* **283**, 346–350.
Sheetz, M. P., Schindler, M. & Koppel, D. E. 1980 Lateral mobility of integral membrane proteins is increased in spherocytic erythrocytes. *Nature, Lond.* **285**, 510–512.
Sheterline, P. & Hopkins, C. R. 1981 Transmembrane linkage between surface glycoproteins and components of the cytoplasm in neutrophils leukocytes. *J. Cell Biol.* **90**, 743–754.
Smith, B. A., Clarke, W. R. & McConnell, H. M. 1979 Anisotropic molecular motion on cell surfaces. *Proc. natn. Acad. Sci. U.S.A.* **76**, 5641–5644.
Stern, P. L. & Bretscher, M. S. 1979 Capping of exogenous Forssman glycolipid on cells. *J. Cell Biol.* **82**, 829–833.
Trinkaus, J. P. 1980 Formation of protrusion of the cell surface during tissue cell movement. In *Tumor cell surfaces and malignancy*, pp. 887–906. New York: Alan R. Liss Inc.
Tsan, M. F. & Berlin, R. D. 1971 Effect of phagocytosis on membrane transport of non-electrolytes. *J. exp. Med.* **134**, 1016–1035.
Walter, R. J., Berlin, R. D. & Oliver, J. M. 1980 Asymmetric Fc receptor distribution of human PMN oriented in a chemotactic gradient. *Nature, Lond.* **286**, 724.
Walter, R. J., Berlin, R. D., Pfeiffer, J. R. & Oliver, J. M. 1980 The polarization of endocytosis and receptor topography on cultured macrophages. *J. Cell Biol.* **86**, 199–211.
Wilkinson, P. C., Michl, J. & Silverstein, S. C. 1980 Receptor distribution in locomoting neutrophils. *Cell. Biol. int. Reps* **4**, 736.
Wolf, D. E., Henkart, P. & Webb, W. W. 1980 Diffusion, patching and capping of stearoylated dextrans on 3T3 cell plasma membranes. *Biochemistry, Wash.* **19**, 3893–3904.

PHILOSOPHICAL TRANSACTIONS OF THE ROYAL SOCIETY B BIOLOGICAL SCIENCES

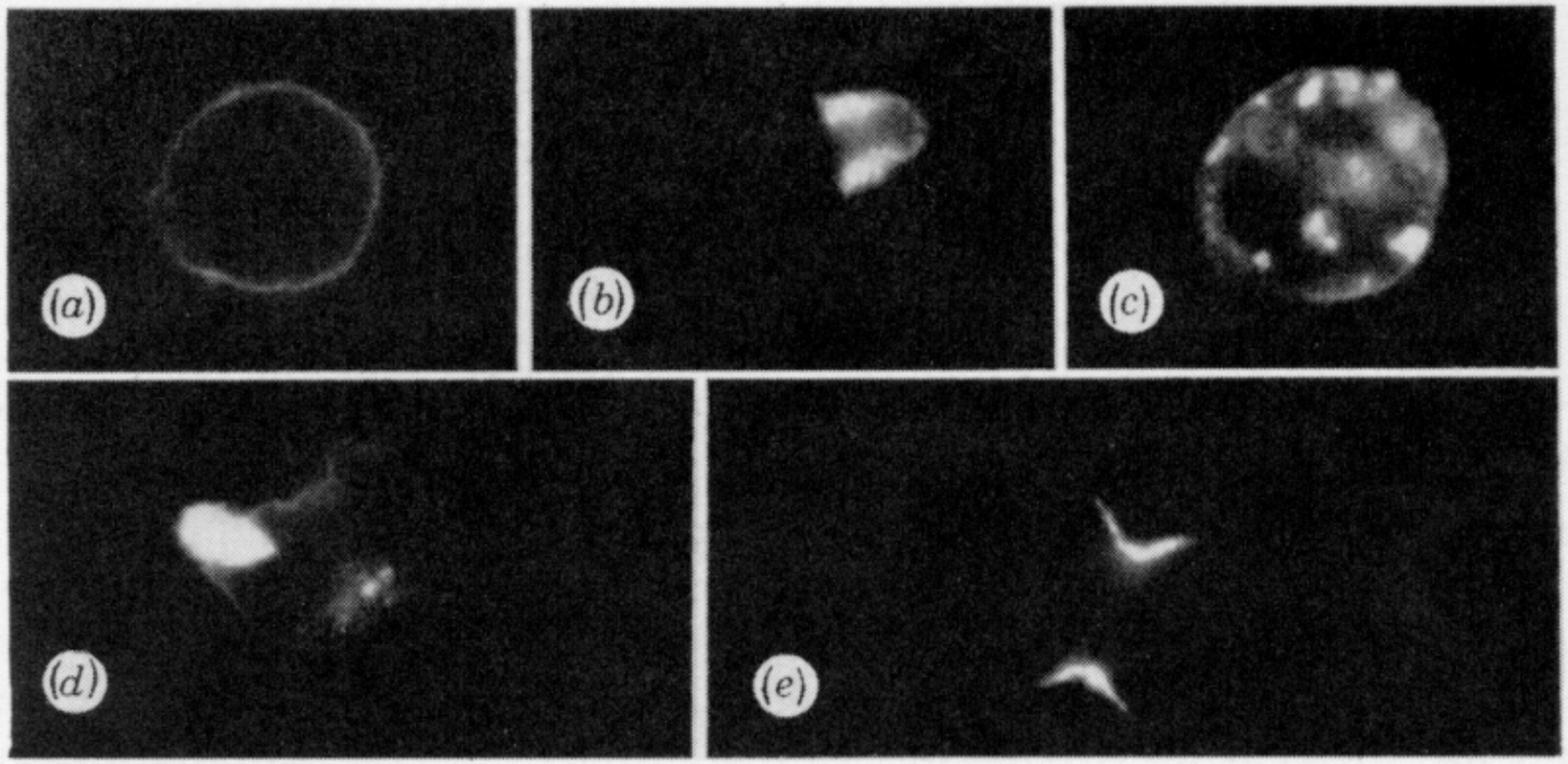

FIGURE 1. The distribution of Con A–receptor complexes on cell surfaces. Variously treated cells were incubated for 5 min at 37 °C with fluorescein-conjugated Concanavalin A (F-Con A) (about 10 μg ml^{-1}). Lectin remains uniformly distributed on untreated cells (*a*). It accumulates in caps on microtubule-depleted (protuberant) cells (*b*), in the pseudopodia of cells performing phagocytosis (*c*), in the uropods of locomoting cells (*d*) and in the cleavage furrow during cytokinesis (*e*). All cells are human polymorphonuclear leukocytes (p.m.ns) except for the mitotic, which is a Chinese hamster ovary cell.

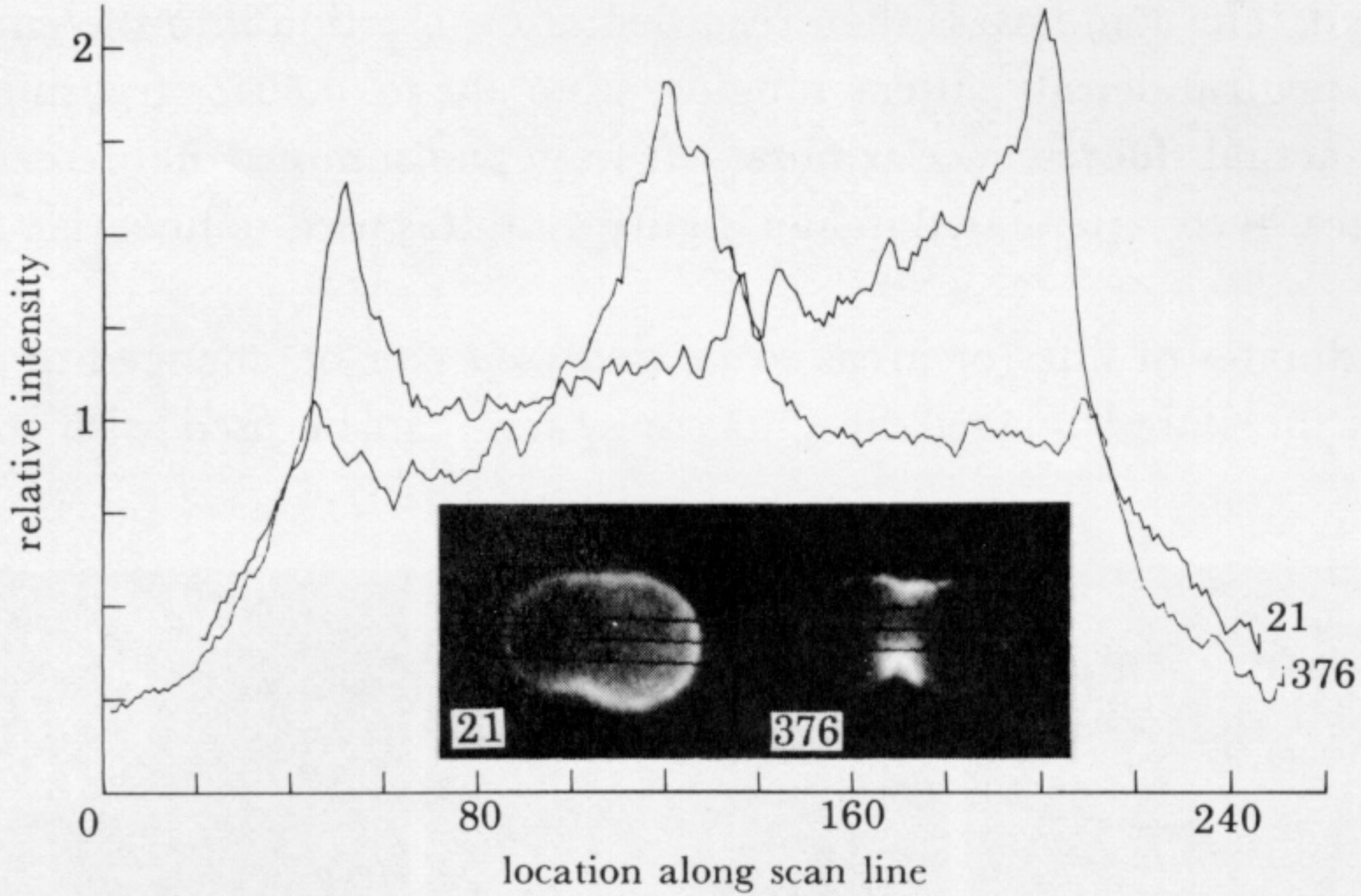

FIGURE 3. Typical QUAVIM scans of the summed F-Con A fluorescence across three lines spanning the long axis of a mitotic macrophage. The cell was labelled at 20 °C. Stage temperature was increased at 37 °C at 30 s. Summed (20 frames) images were selected in early anaphase (21 s) and late telophase (376 s). The photographs show the geometry of the cell at each point and the position of the scan lines.

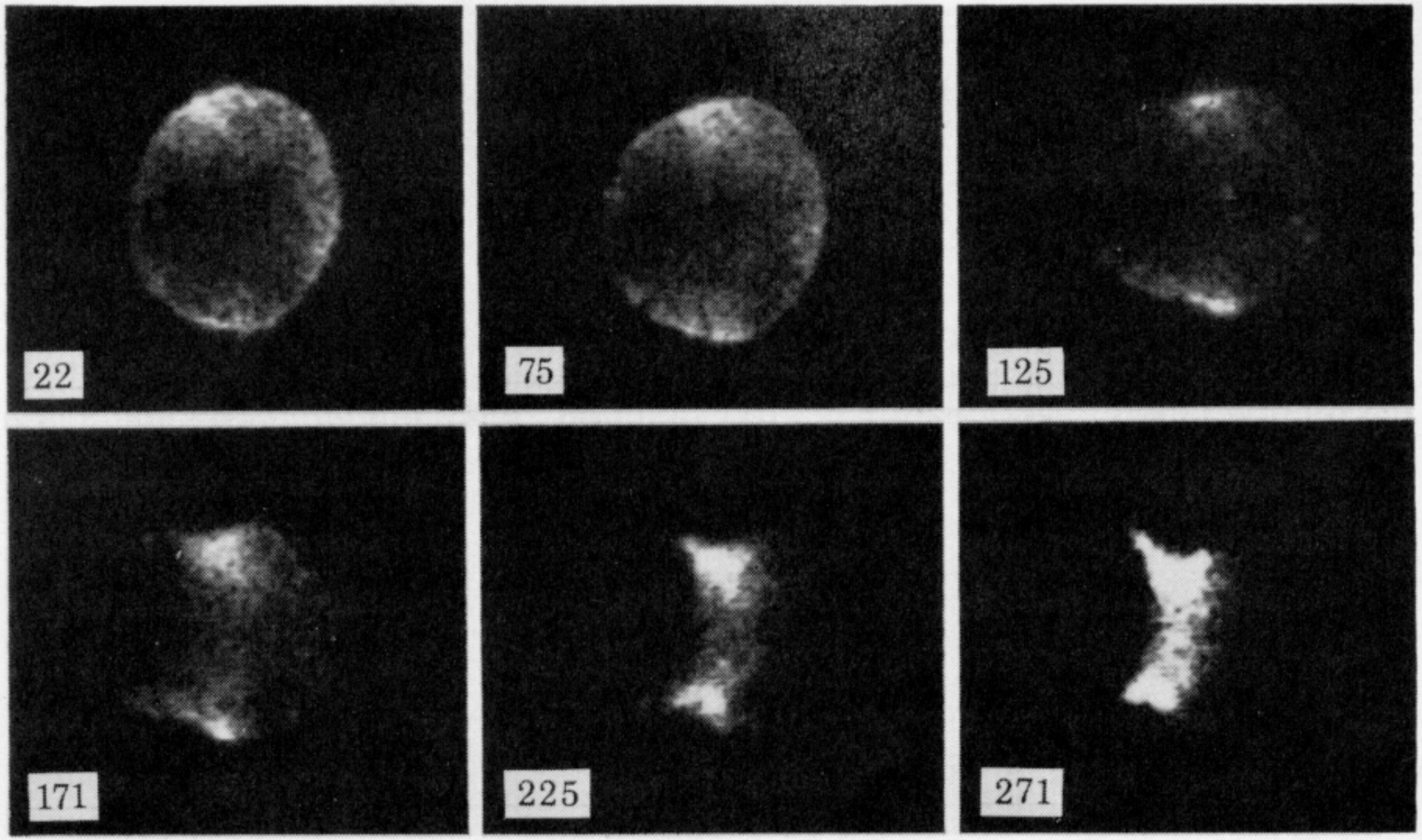

FIGURE 5. Frames from a video recording of a J774.2 macrophage labelled for 1 min at 37 °C with FS-Con A, selected for observation by epifluorescence illumination and viewed through an image intensification television camera. The distribution of fluorescence was recorded from metaphase through early G_1 by tape recording and subsequent transfer of selected processed (64 frame averaged) frames to a Tektronix 634 monitor for photography using Tri-X-Pan film in a Tektronix C-28 camera. Time is given in seconds.

PHILOSOPHICAL TRANSACTIONS OF THE ROYAL SOCIETY B BIOLOGICAL SCIENCES

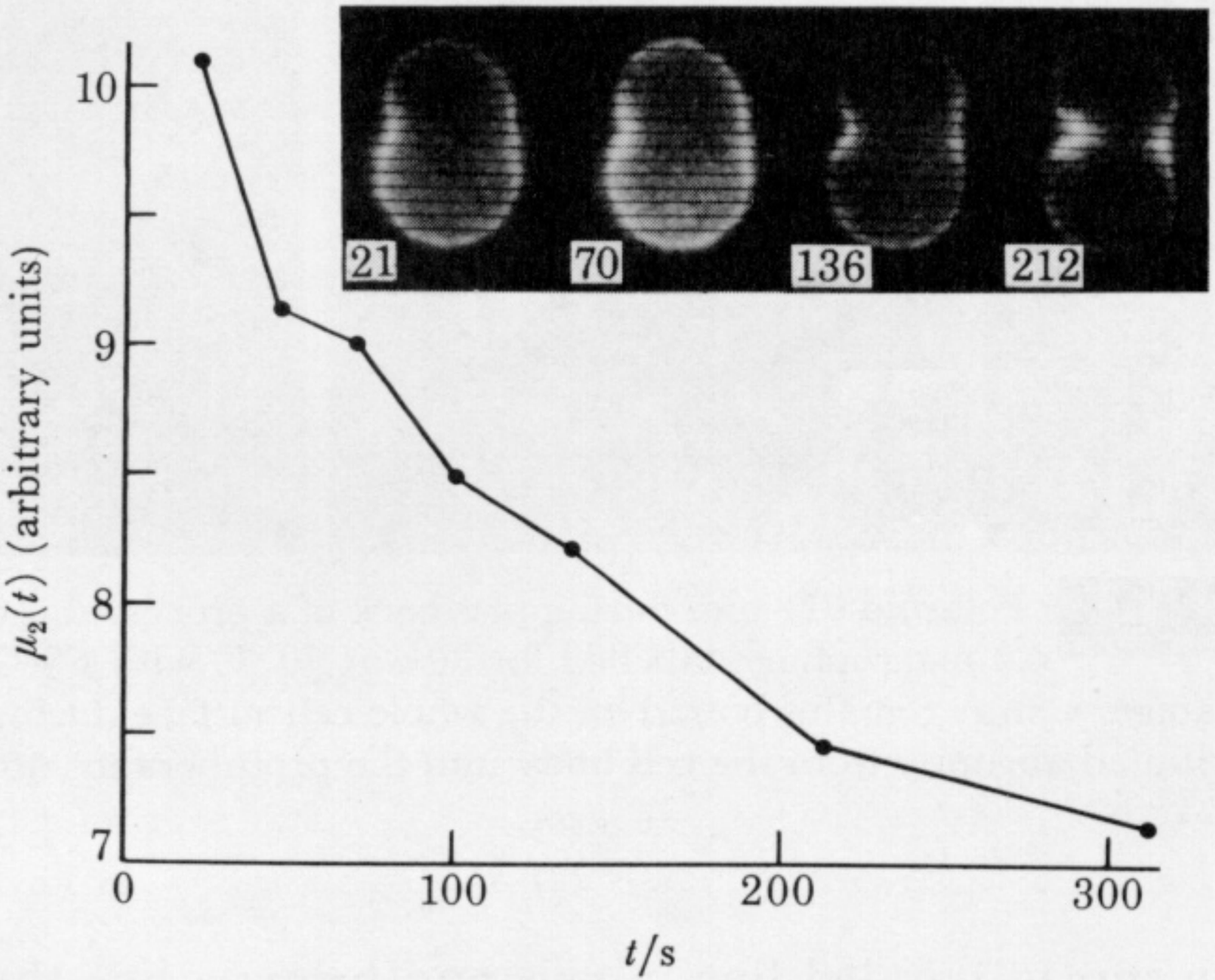

FIGURE 9. Time course of calculated $\mu_2(t)$ for the distribution of F-Con A fluorescence for a J774.2 macrophage followed from early anaphase to late telophase. Summed (15 frames) images were grabbed and digitized in the image processor. Fluorescence intensity readings were then taken across the series of equally spread parallel lines, seven above and seven below a line through the cleavage furrow. Second moments were calculated from the summed intensities across each line. The plot incorporates data from seven sequential frames. Photographs of distribution of fluorescence and location of the lines are shown for four of the seven frames.

PHILOSOPHICAL TRANSACTIONS OF THE ROYAL SOCIETY B BIOLOGICAL SCIENCES

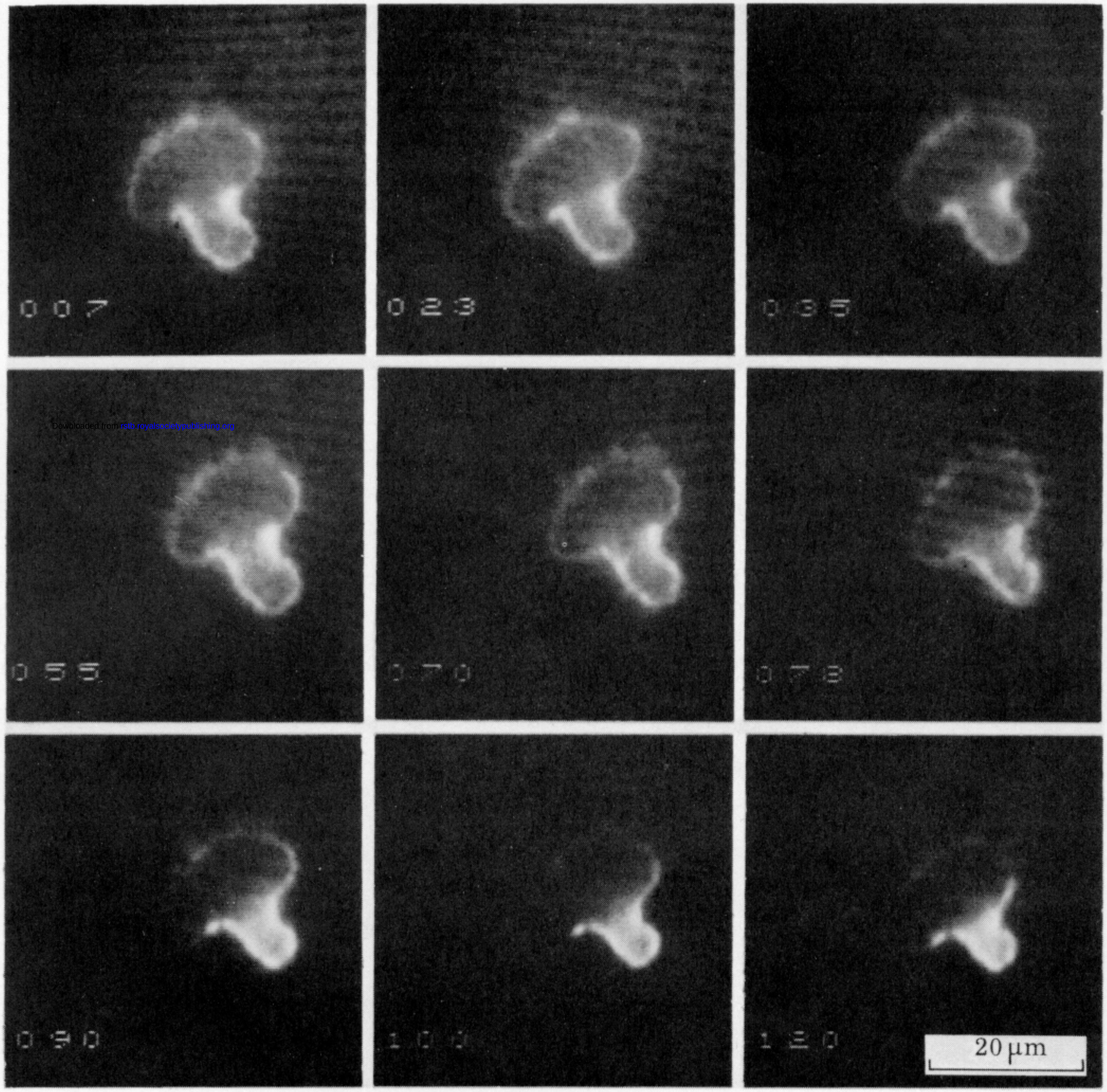

FIGURE 10. Frames photographed on Polaroid 611 film during playback of a processed (16 frame averaging) video recording of a protuberant J774.2 macrophage labelled for 30 s at 20 °C with FS-Con A then incubated at 37 °C on a microscope stage. Con A remains bound on the whole cell surface during approximately 0.5 min at 37 °C, then is redistributed abruptly from the cell body into the protuberance during a period of 10–20 s. Bar = 20 μm.

PHILOSOPHICAL TRANSACTIONS OF THE ROYAL SOCIETY B BIOLOGICAL SCIENCES
PHILOSOPHICAL TRANSACTIONS OF THE ROYAL SOCIETY B BIOLOGICAL SCIENCES

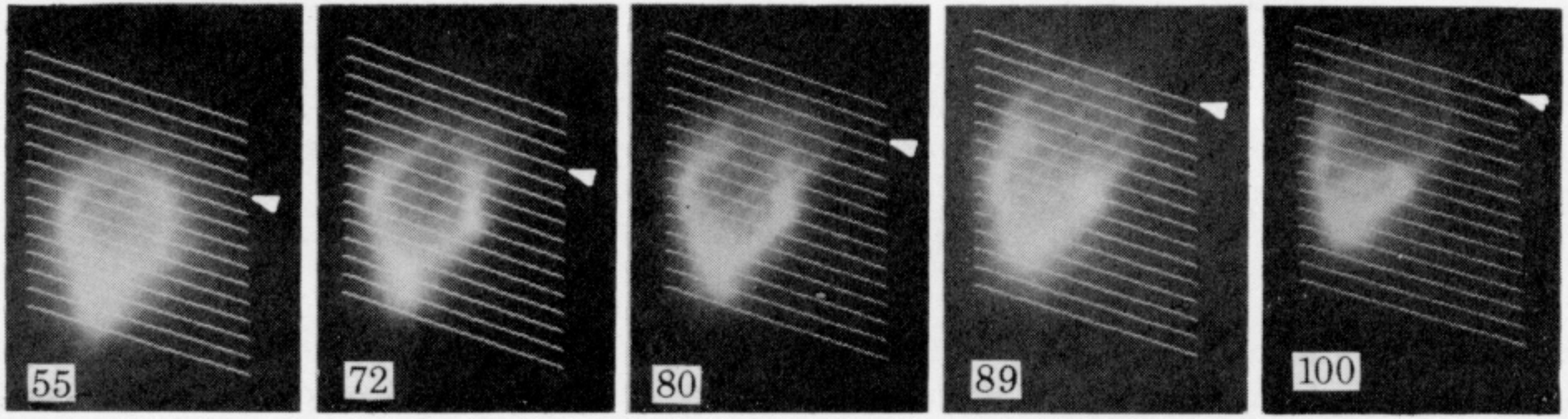

FIGURE 12. Frames photographed on Polaroid 611 film during playback of a processed (15 frame summation) video film of a F-Con A-labelled locomoting p.m.n. Cell monolayers were oriented by incubation at 37 °C for 15 min with 0.5 μM f-Met-Leu-Phe, then labelled at 10 °C for 30 s with 100 μg ml^{-1} F-Con A. A polarized cell was selected for observation at 10 °C and the stage temperature was increased to 25 °C at 45 s on this recording. A rapid clearing of fluorescence from the lamellipodium towards the uropod was observed. In this figure, a grid composed of 15 lines at 1.5 μm intervals is superimposed on each 15-summed frame by use of the LM^2 computer. Fluorescence intensity across each line was transferred to computer memory for further analysis. The arrowheads indicate the line across the lamellipodial tip (0 μm) for each frame. The total fluorescence intensity summed between lines 1 and 15 was essentially unchanged from frames 55 to 100, indicating relatively little loss of fluorescence due to bleaching, self-adsorption, saturation or other sources within this experiment (data not shown). Bar = 10 μm.

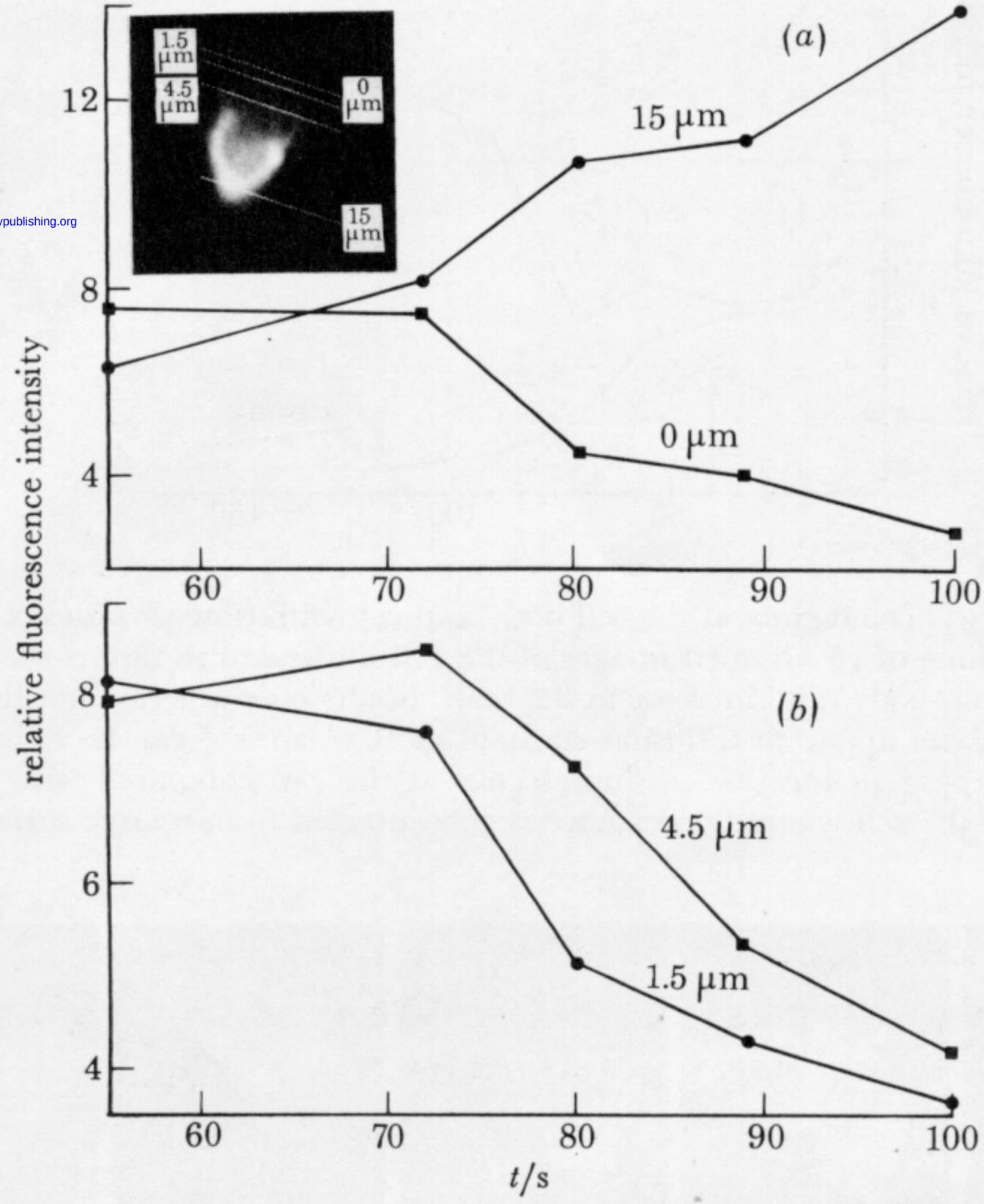

FIGURE 13. Summed fluorescence intensities with time of selected lines across a F-Con A-labelled, locomoting p.m.n. In (*a*), fluorescence intensity was summed across lines at 0 μm (lamellipodial tip) and 15 μm (uropod). In (*b*), fluorescence intensity was summed across lines at 1.5 μm and 4.5 μm behind the lamellipodium. The inset shows the position of these four lines at one time point (80 s).

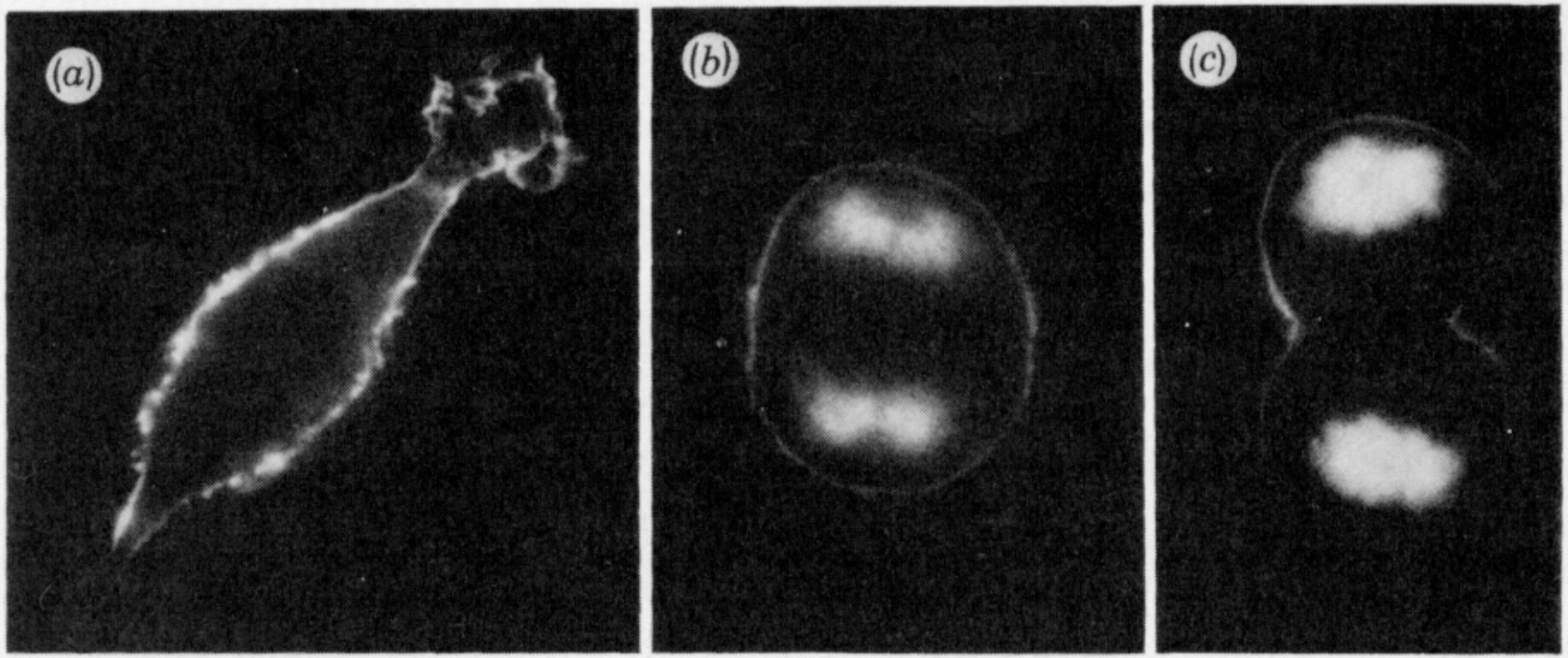

FIGURE 14. Distribution of F-CTB on J774.2 macrophages. Cell monolayers were incubated at 37 °C for 10 min with F-CTB, then fixed with 4% paraformaldehyde and incubated with Hoechst 33258, a DNA-binding dye that simplifies location of mitotic cells. The fluorescent ligand outlines the most delicate membrane folds and ruffles of the interphase cell (*a*). The regions of increased intensity most likely indicate regions of increased membrane accumulation. A remarkably uniform distribution of F-CTB fluorescence is seen at early anaphase before formation of the cleavage furrow (*b*). This essentially uniform labelling persists at late anaphase with only a hint of increased fluorescence intensity at the cleavage furrow (*c*).

PHILOSOPHICAL TRANSACTIONS OF THE ROYAL SOCIETY B BIOLOGICAL SCIENCES

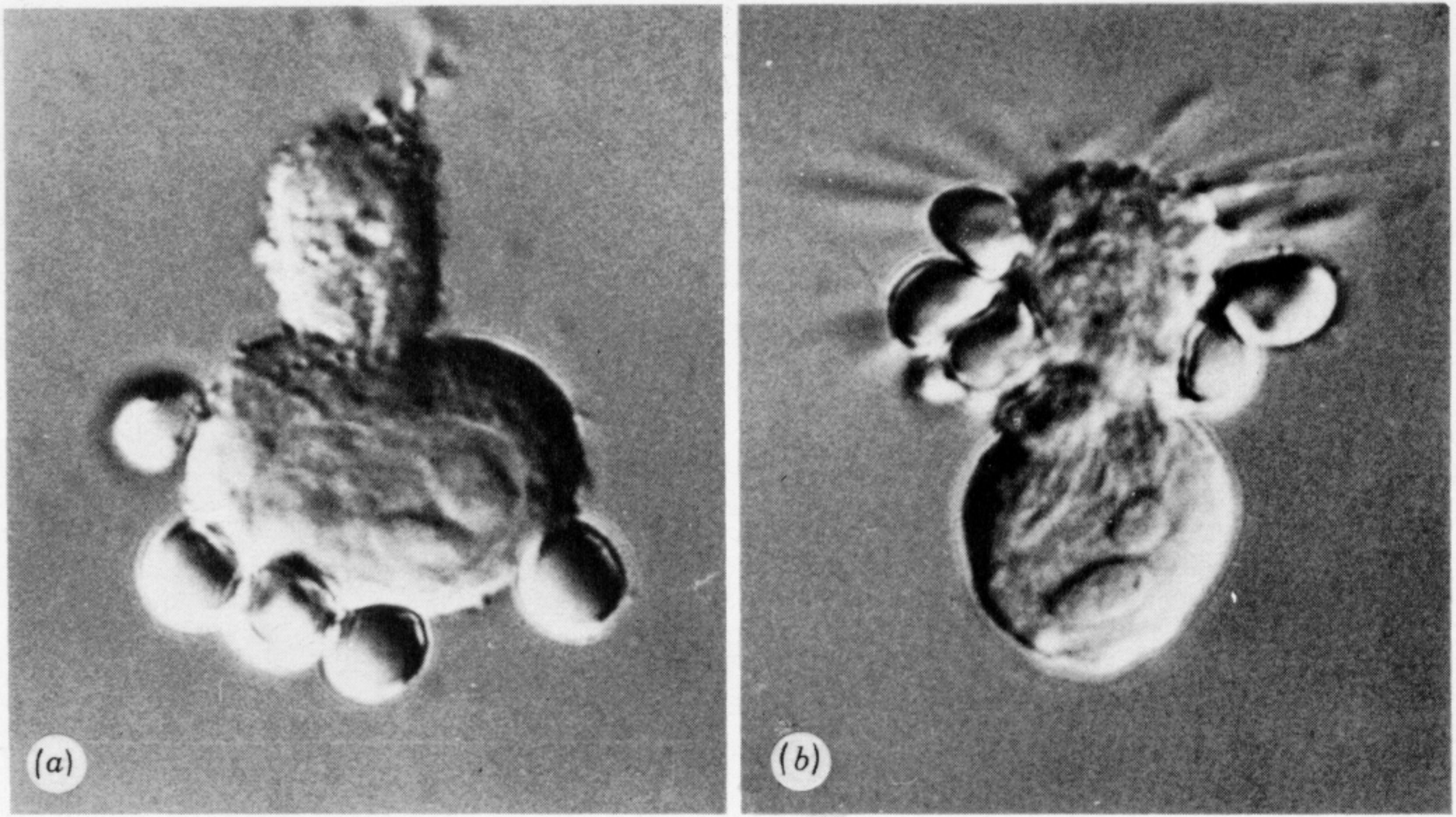

FIGURE 15. The distribution of complement-opsonized erythrocytes on colchicine-treated macrophages. After 45 s at 37 °C, erythrocytes are bound at the nuclear pole of the cell (*a*). They redistribute to the protuberance after rinsing and further incubation for 5 min or more at 37 °C (*b*).

PHILOSOPHICAL TRANSACTIONS OF THE ROYAL SOCIETY B BIOLOGICAL SCIENCES

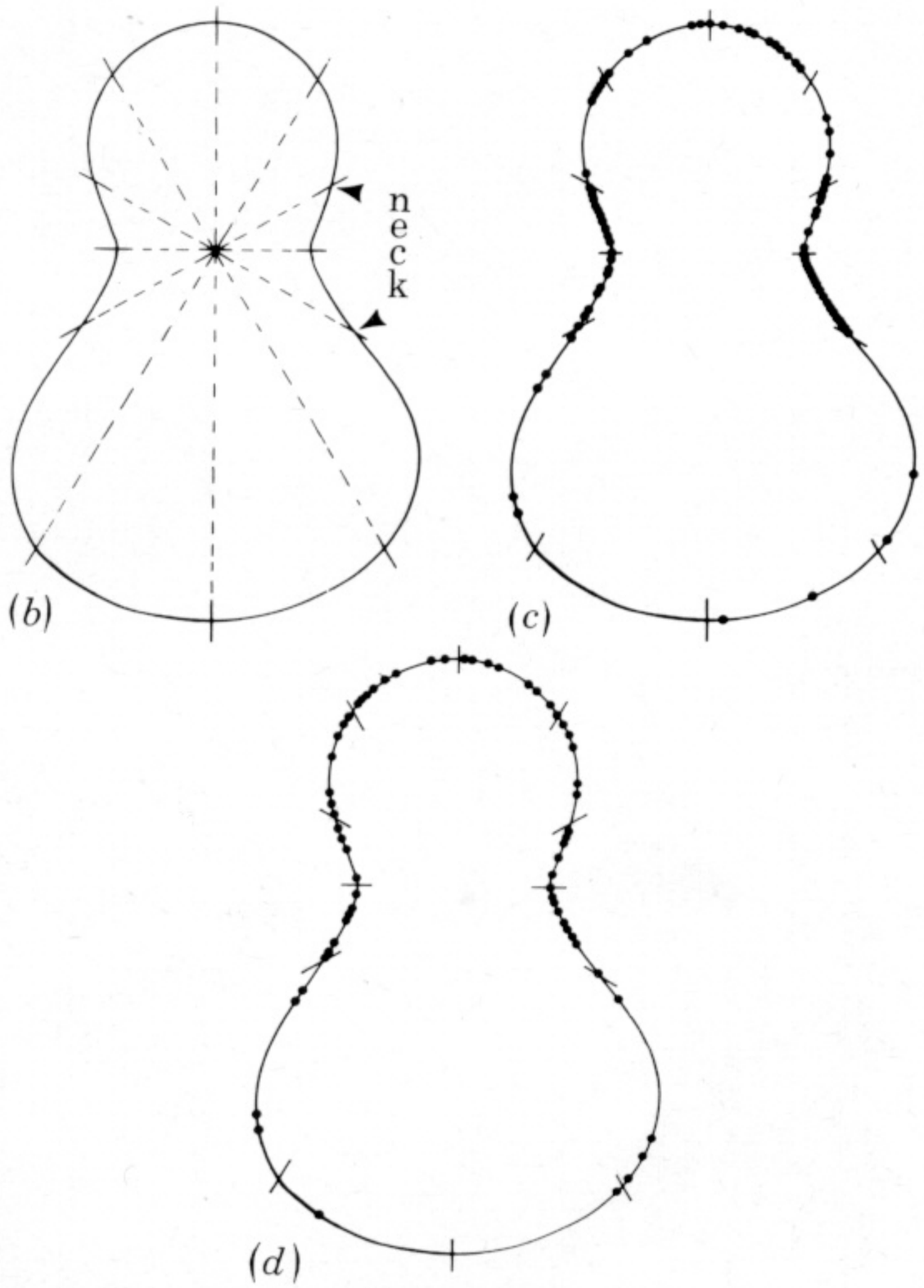

FIGURE 16. The distribution of coated pits on protuberant cells. A cumulative map of coated pit topography was built by translocating pits from individual electron micrographs (*a*) onto equivalent quadrats (equal-length segments along the surface profile) of a diagrammatic cell (*b*) whose dimensions were proportional to those of the original cell. The results of two typical experiments, each analysing 12 randomly chosen protuberant J774.2 macrophages from colchicine-treated (10 μm, 60 min) populations, are given in (*c*) and (*d*). They demonstrate the concentration of pits in the 'neck' and 'head' regions of protuberant cells.

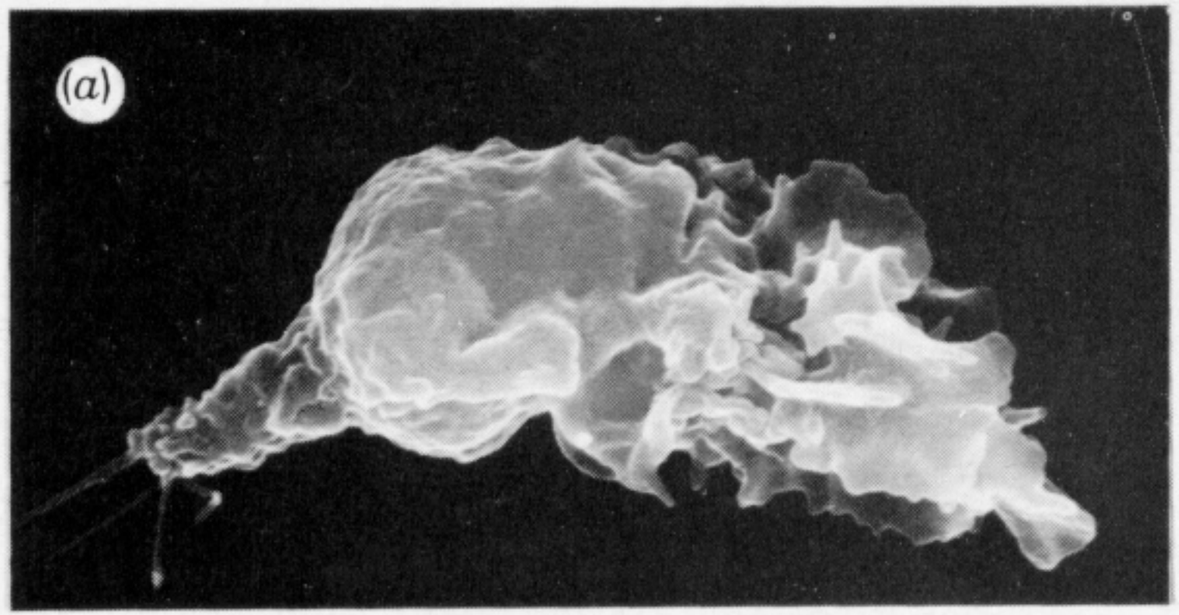

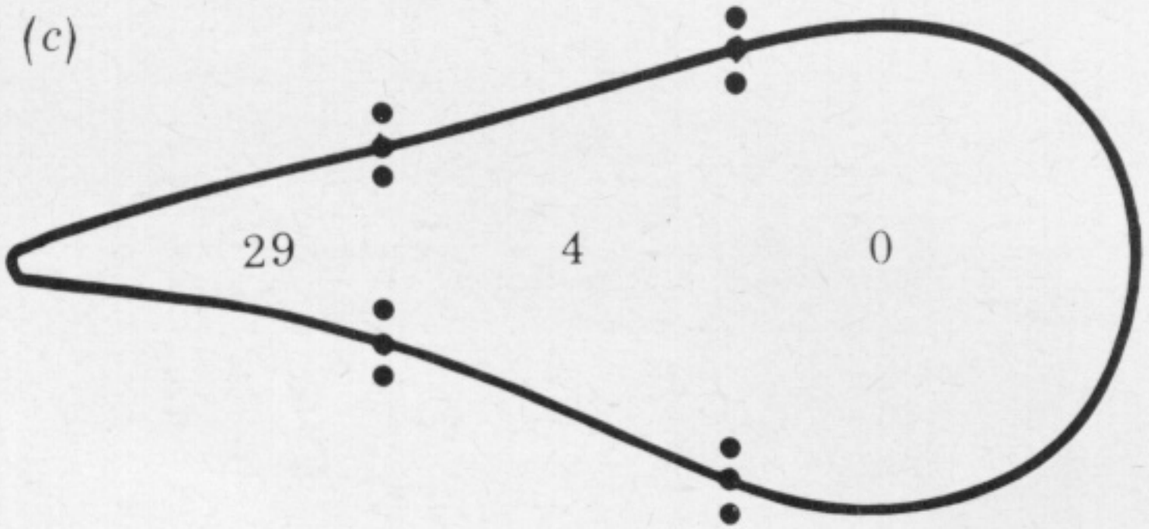

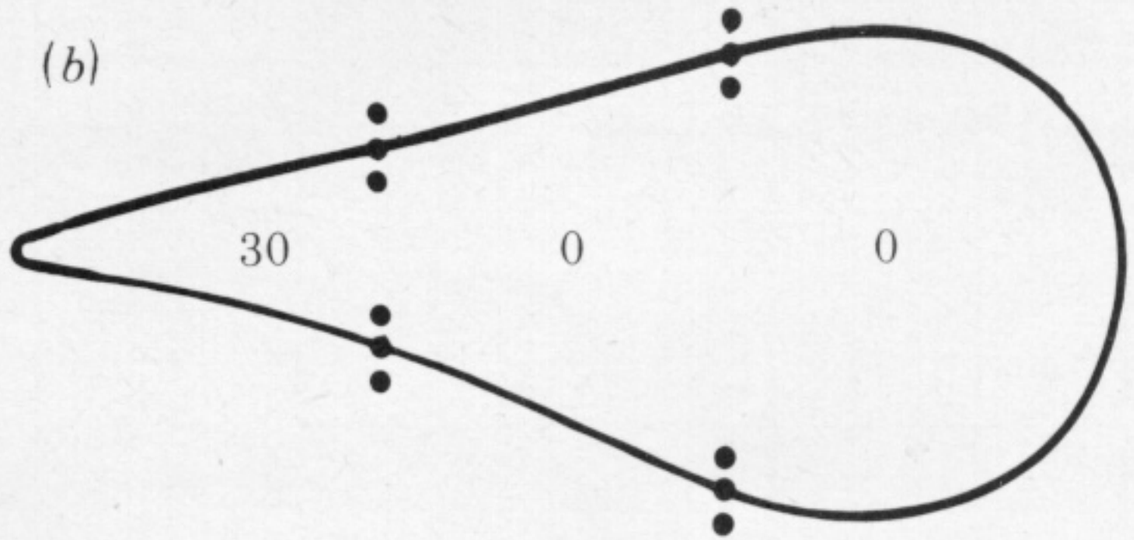

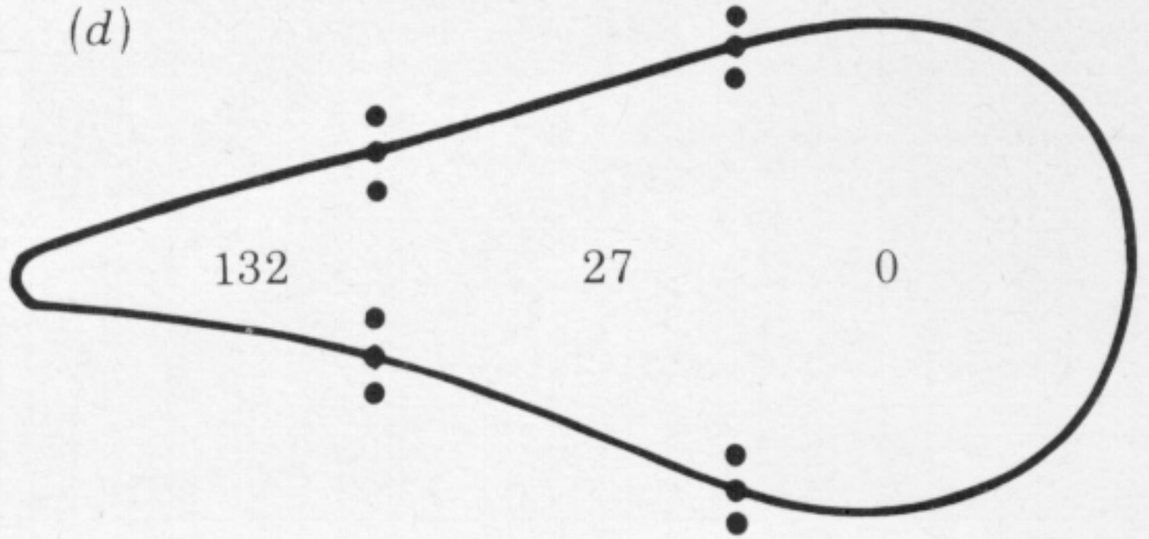

FIGURE 17. The topography of coated pits and coated vesicles during chemotaxis in human p.m.ns. The numbers of coated pits (*b*, *c*) or pits and coated vesicles (*d*) occupying the anterior, central or posterior thirds of the total cell perimeter were determined in human p.m.ns polarized by 20 min incubation in a gradient (*a*, *c*) or in suspension (*b*) with f-Met-Leu-Phe (0.1 μM). The results in (*b*) were obtained by analysis of 10 cells from two separate experiments; (*c*) is from 16 cells from two experiments; and (*d*) analyses 17 cells from three experiments; (*a*) illustrates the typical polarized morphology of locomoting p.m.ns. (S.e.m.; magn. × 4500.)

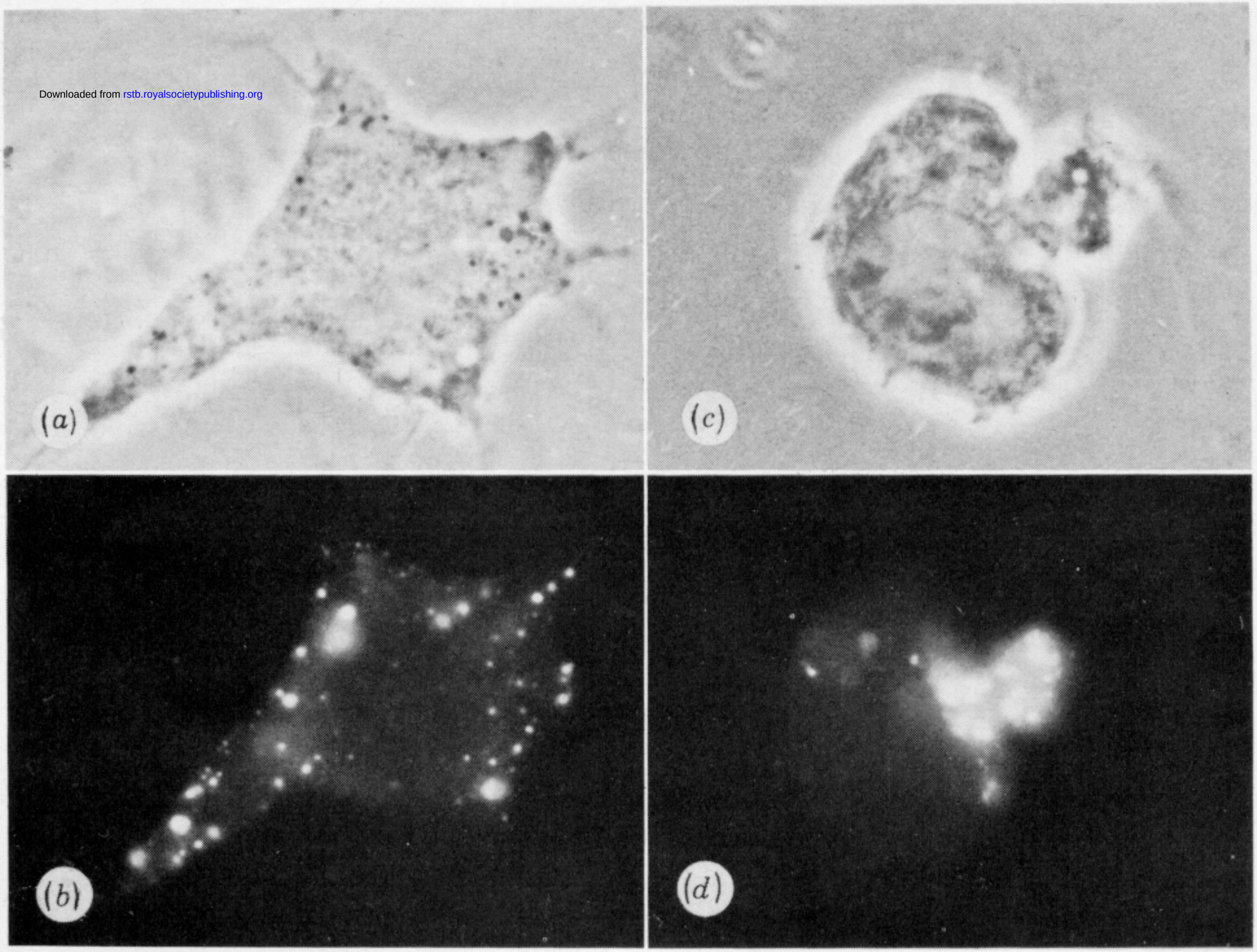

FIGURE 18. The topographical restriction of pinocytosis in protuberant macrophages. The untreated, spread macrophage ingests fluorescein-dextran by fluid pinocytosis from points over the whole surface (*a*, *b*). In contrast, fluorescein-dextran uptake is confined to the protuberance of the colchicine-treated cell. Both cells were incubated at 37 °C for 5 min with 5 mg ml^{-1} fluorescein-dextran.

PHILOSOPHICAL TRANSACTIONS OF THE ROYAL SOCIETY B BIOLOGICAL SCIENCES